JCI The Journal of Clinical Investigation

Developmental endothelial locus-1 protects from hypertension-induced cardiovascular remodeling via immunomodulation

Theresa Failer, … , Vladimir Todorov, Irakli Kopaliani

J Clin Invest. 2022. https://doi.org/10.1172/JCI126155.

Research In-Press Preview **Cardiology** **Inflammation**

The causative role of inflammation in hypertension-related cardiovascular diseases is evident and calls for development of specific immunomodulatory therapies. We tested the therapeutic efficacy and mechanisms of action of developmental endothelial locus-1 (DEL-1), an endogenous anti-inflammatory factor, in angiotensin-II (ANGII)- and DOCA (deoxycorticosterone acetate)-salt-induced cardiovascular organ damage and hypertension. By using mice with endothelial overexpression of DEL-1 (EC-Del1) and performing preventive and interventional studies by injecting recombinant DEL-1 in mice, we showed that DEL-1 improved endothelial function and abrogated aortic adventitial fibrosis, medial thickening and loss of elastin. DEL-1 also protected the mice from cardiac concentric hypertrophy, interstitial and perivascular coronary fibrosis and improved left-ventricular function and myocardial coronary perfusion. DEL-1 prevented aortic stiffness and abolished the progression of hypertension. Mechanistically, DEL-1 acted by inhibiting αvβ3-integrin dependent activation of pro-MMP2 in mice and in human isolated aorta. Moreover, DEL-1 stabilized αvβ3-integrin dependent CD25+FoxP3+ Treg numbers and IL-10 levels, which were associated with decreased pro-inflammatory cell recruitment of inflammatory cells and reduced production of pro-inflammatory cytokines in cardiovascular organs. The demonstrated effects and immune-modulating mechanisms of DEL-1 in abrogation of cardiovascular remodeling and progression of hypertension identify DEL-1 as a potential therapeutic factor.

Developmental endothelial locus-1 protects from hypertension-induced cardiovascular remodeling via immunomodulation

Theresa Failer[1*], Michael Amponsah-Offeh[1*], Aleš Neuwirth[2], Ioannis Kourtzelis[2,3], Pallavi Subramanian[2], Peter Mirtschink[2], Mirko Peitzsch[2], Klaus Matschke[4], Sems M. Tugtekin[4], Tetsuhiro Kajikawa[5], Xiaofei Li[5], Anne Steglich[6], Florian Gembardt[6], Annika Wegner[6], Christian Hugo[6], George Hajishengallis[5], Triantafyllos Chavakis[2], Andreas Deussen[1], Vladimir Todorov[6], Irakli Kopaliani[1]

[1] Department of Physiology, Medical Faculty Carl Gustav Carus, Technische Universität Dresden, Dresden, Germany

[2] Institute for Clinical Chemistry and Laboratory Medicine, Medical Faculty Carl Gustav Carus, Technische Universität Dresden, Dresden, Germany

[3] Hull York Medical School, York Biomedical Research Institute, University of York, York, YO10 5DD, UK

[4] Department of Cardiac Surgery, Heart Center Dresden GmbH, Medical Faculty Carl Gustav Carus, Technische Universität Dresden, Dresden, Germany

[5] University of Pennsylvania, Penn Dental Medicine, Department of Basic and Translational Sciences, Philadelphia, Pennsylvania, USA

[6] Experimental Nephrology, Division of Nephrology, Department of Internal Medicine III, University Hospital Carl Gustav Carus, Technische Universität Dresden, Dresden, Germany

* These authors contributed equally

Corresponding author: Jun-Prof. Dr. Irakli Kopaliani
Department of Physiology
Medical Faculty Carl Gustav Carus
Technische Universität Dresden, Germany
Fetscherstr. 74
01307
Phone: +49 351 4586030
Fax: +49 351 4586301
Email: irakli.kopaliani@tu-dresden.de

Conflict of interest

The authors have declared that no conflict of interest exists

Abstract

The causative role of inflammation in hypertension-related cardiovascular diseases is evident and calls for development of specific immunomodulatory therapies. We tested the therapeutic efficacy and mechanisms of action of developmental endothelial locus-1 (DEL-1), an endogenous anti-inflammatory factor, in angiotensin II (ANGII)- and DOCA (deoxycorticosterone acetate)-salt-induced cardiovascular organ damage and hypertension. By using mice with endothelial overexpression of DEL-1 (EC-Del1) and performing preventive and interventional studies by injecting recombinant DEL-1 in mice, we showed that DEL-1 improved endothelial function and abrogated aortic adventitial fibrosis, medial thickening and loss of elastin. DEL-1 also protected the mice from cardiac concentric hypertrophy, interstitial and perivascular coronary fibrosis and improved left-ventricular function and myocardial coronary perfusion. DEL-1 prevented aortic stiffness and abolished the progression of hypertension. Mechanistically, DEL-1 acted by inhibiting αvβ3-integrin dependent activation of pro-MMP2 in mice and in human isolated aorta. Moreover, DEL-1 stabilized αvβ3-integrin dependent CD25+FoxP3+ Treg numbers and IL-10 levels, which were associated with decreased pro-inflammatory cell recruitment of inflammatory cells and reduced production of pro-inflammatory cytokines in cardiovascular organs. The demonstrated effects and immune-modulating mechanisms of DEL-1 in abrogation of cardiovascular remodeling and progression of hypertension identify DEL-1 as a potential therapeutic factor.

Brief Summary

Del-1 abrogates hypertension-induced cardiovascular remodeling and progression of hypertension by suppressing inflammation via stabilizing anti-inflammatory Treg/IL-10 responses and inhibition of pro-MMP2 activation in target organs.

Introduction

Hypertension is a major risk factor for development of cardiovascular diseases, which cause the highest number of deaths worldwide among non-infectious diseases (1). Currently, over one billion adults are affected by hypertension and this number is projected to rise (1). Therefore, hypertension-caused cardiovascular diseases will remain a global health problem and a major socio-economical healthcare burden. During hypertension, aorta undergoes fibrosis and hypertrophy, along with degradation of elastic fibers and dilatation and leads to its stiffening (2). Aortic stiffening considerably increases afterload and leads to progressive increase in systolic blood pressure (SBP), adversely affecting circulation in brain, kidney and heart by that increasing the incidence of stroke, renal failure and myocardial infarction (3). Hypertension and aortic stiffness also contribute to development of cardiac remodeling, resulting in left ventricular (LV) hypertrophy, and fibrosis, in turn adversely affecting cardiac relaxation and coronary perfusion, along with forced reduction of oxidative metabolism and increased reliance on glucose. Altogether, these pathological changes in the heart may result in cardiac failure (3, 4).

Although pathophysiological mechanisms of hypertension and associated cardiovascular diseases are not fully understood, excessive activation of the renin-angiotensin-aldosterone system and production of angiotensin II (ANGII) are critically involved (5). ANGII increases arterial pressure by inducing strong vasoconstriction and promotion of sodium und water reuptake (via aldosterone) from the renal tubules. While increased arterial pressure may contribute to cardiovascular organ damage, solid evidence indicates a critical direct role of inflammation in the development of hypertension and cardiovascular organ damage. Initial leukocyte recruitment of the innate immune system followed by T-cell-driven inflammation and excessive IL-17 production mediate ANGII-induced cardiovascular remodeling and development of hypertension (6–12). In the deoxycorticosterone acetate (DOCA)-salt model (hypervolemic hypertension induced by excessive renal salt retention) activated T-cells and pro-inflammatory cytokines (e.g. IFN-γ, IL-17, and IL-18) are also involved in the pathogenesis of the hypertensive disorder and organ damage (13). Increase in arterial pressure and direct ANGII stimulation, both promote pro-inflammatory CD4+ and CD8+ T-cell immune response in cardiovascular tissues. Subset of pro-inflammatory CD4+ T cells, e.g. Th17 cells produce IL-17, which in turn mediates cardiovascular remodeling. Gene knockout of IL-17 or neutralization with antibodies limit hypertension-induced inflammatory target organ damage and progression of hypertension (10–12, 14). The pro-inflammatory profile during ANGII-induced hypertension is accompanied by destabilized and reduced anti-inflammatory CD4+FoxP3+ regulatory T-cell (Treg) response, along with a decrease in IL-10 production (14–18). This aggravates hypertension-induced inflammatory cardiovascular organ

damage. Restoration of Treg response or supplementation of IL-10 protects from this damage both in vessels and heart (15–17, 19–21). Along with inflammation, cardiovascular remodeling during hypertension is accompanied with an increased matrix metalloproteinase-2 (MMP2) activity (22–24). In aorta, MMP2 is released as a latent 72 kDa pro-MMP2 from smooth muscle cells (SMCs) and activated in an αvβ3-integrin-dependent process by catalytic cleavage of the pro-domain and activation to 62-kDa MMP2 (25). While αvβ3-integrin engages pro-MMP2 on the cell membrane, furin activated membrane type 1 MMP (MT1-MMP) catalytically cleaves it (25). We previously demonstrated that activation of pro-MMP2 in aorta is endothelium/endothelin-1 (ET1) dependent. Endothelium-released ET1 regulates furin activity in smooth muscle cells, which in turn controls MT1-MMP activity and ultimately activation of latent pro-MMP2 (26, 27). In heart, ANGII also stimulates release of pro-MMP-2 from cardiac fibroblasts and cardiomyocytes followed by catalytic activation by MT1-MMP (25). MMP2 is capable of degrading elastic fibers in aorta and its activity is critically associated with aortic remodeling and an increase in its stiffness (22). MMP2 activities also contribute to cardiac hypertrophy and fibrosis (22).

Current treatment strategies to limit cardiovascular damage during hypertension are aimed on lowering arterial pressure, especially by inhibition of renin-angiotensin-system by angiotensin converting enzyme inhibitors or angiotensin type 1 receptor antagonists (1). However, strong evidential implications of inflammation in hypertension-induced cardiovascular diseases call for testing novel anti-inflammatory strategies as a new approach for better management of hypertension-induced cardiovascular or other organ damage, along with lowering arterial pressure. In this regard, inhibition of leukocyte recruitment and stabilizing/increasing anti-inflammatory Treg cell numbers are considered as potential anti-inflammatory therapeutic approaches to limit target organ damage and progression of hypertension.

Developmental endothelial locus-1 (DEL-1) is an endogenous anti-inflammatory glycoprotein expressed and secreted by many cell types including endothelial cells (28–30). DEL-1 is highly expressed in immune privileged organs, with a relatively low expression in cardiovascular tissues (28, 31, 32). Previously, we have shown that DEL-1 inhibits leukocyte recruitment and most importantly IL-17-dependent pathologies (28, 29, 33, 34). Its efficacy has been tested in IL-17-mediated inflammatory bone loss in mice and primates, as well as in a mouse model of multiple sclerosis (28, 33, 34). Besides leukocyte recruitment, DEL-1 exerts its immunomodulatory actions via resolution of inflammation by efferocytosis and induction of anti-inflammatory Treg response (35, 36). The anti-recruitment action of DEL-1 is mediated via inhibition of β2-integrin/ICAM interaction, whereas efferocytosis and induction of Treg response are mediated via interaction of DEL-1 to αvβ3-integrin by its RGD sequence in the second EGF-repeat (29, 37). Thus, DEL-1 can

resolve IL-17-mediated pathologies, such as inflammatory bone loss and multiple sclerosis by suppressing inflammation with various anti-inflammatory actions, which depend on interaction of DEL-1 with integrins. However, whether the anti-inflammatory properties of DEL-1 can prevent hypertension-related cardiovascular organ damage has not been hitherto addressed. Furthermore, it is unknown whether additional immunomodulatory actions of DEL-1 can be critical for prevention of the organ damage during hypertension. In that regard, because DEL-1 interacts with αvβ3 integrin, it was of particular interest to investigate whether DEL-1 interferes with the activation of pro-MMP2. Therefore, we investigated the efficacy and mechanisms of action of DEL-1 in ANGII- and DOCA-salt-induced inflammatory cardiovascular remodeling and progression of hypertension. For this, we performed experiments in a mouse model overexpressing endothelium-specific DEL-1 and to obtain interventional proof, performed three different therapeutic studies by application of recombinant soluble DEL-1 in WT mice, complemented with multiple human and mouse cell culture and isolated tissue experiments.

Results

DEL-1 overexpression protects from ANGII-induced aortic and cardiac structural and metabolic remodeling

Major parameters of aortic remodeling, such as adventitial collagen, medial thickness and elastin content were assessed after 4-weeks infusions of ANGII or vehicle. After ANGII infusion, WT mice had higher adventitial collagen (P<0.01, Figure 1A, D) and medial thickness (P<0.01, Figure 1B, E), along with lower elastin area (P<0.01, Figure 1C, F) compared to vehicle-infused WT mice. Compared to ANGII-infused WT mice, EC-Del1 mice had less adventitial collagen (P<0.01, Figure 1A, D) and lower medial thickness (P<0.01, Figure 1B, E), as well as more elastin (P<0.01, Figure 1C, F) after ANGII infusion. Cardiac remodeling was evaluated by assessment of LV lumen-to-wall ratio and cross-sectional area of cardiomyocytes, as well as interstitial and perivascular collagen depositions. Compared to vehicle, ANGII-infused WT mice developed cardiac remodeling, resulting in decreased LV lumen-to-wall ratio (P<0.01, Figure 1G, K) and increased cardiomyocyte area (P<0.01, Figure 1H, L), along with profound deposition of interstitial (P<0.01, Figure 1I, M) and perivascular collagen (P<0.01, Figure 1J, N,). Compared to ANGII-infused WT mice, EC-Del1 mice had higher LV lumen-to-wall ratio (P<0.01, Figure 1G, K) and lower cardiomyocyte area (P<0.01, Figure 1H, L), as well as less interstitial (P<0.01, Figure 1I, M) and perivascular collagen deposition (P<0.01, Figure 1J, N,) after ANGII infusion.

Cardiac function was further evaluated and compared between groups with echocardiography and isolated perfused heart experiments. Compared to vehicle, ANGII-infused WT mice showed typical characteristics of pathological concentric hypertrophic cardiomyopathy expressed by increase in LV wall thickness during diastole (P<0.01, Figure 2A, E, F) and systole (P<0.01, Figure 2B, E, F), along with decreased end-diastolic (P<0.01, Figure 2C) and stroke volumes (P<0.01, Figure 2D). Compared to ANGII-infused WT mice, EC-Del1 mice showed lower LV wall thickness during diastole (P<0.01, Figure 2A, E, F) and systole (P<0.05, Figure 2B, E, F), along with higher end-diastolic (P<0.05, Figure 2C) and stroke volumes (P<0.01, Figure 2D). Compared to vehicle, ANGII-infused WT mice showed an increase in heart mass (P<0.01, Figure 3A) and reduction in coronary flow reserve in response to a flow stop (P<0.01, Figure 3B) and adenosine infusion (P<0.01, Figure 3C). This was accompanied with a decrease in mRNA levels of adenosine type 1 (P<0.01, Figure 3D), 2a (P<0.01, Figure 3E) and 2b (P<0.01, Figure 3F), but not type 3 (Figure 3G) receptors. We furthermore assessed cardiac metabolic adaptation after ANGII infusion by evaluation of glucose metabolism. For this, effluents from perfused hearts were collected for assessment of several metabolites. Compared to vehicle, hearts of ANGII-infused WT mice showed higher lactate (P<0.01, Figure 3H) and malate (P<0.01, Figure 3I), whereas ANGII-infused

EC-Del1 mice had lower lactate (P<0.01, Figure 3H) and malate (P<0.01, Figure 3I). Pyruvate did not differ between the groups (Figure 3J).

DEL-1 overexpression protects from ANGII-induced progression of hypertension and endothelial dysfunction

We next assessed the effects of DEL-1 on development of SBP during 4-weeks of ANGII infusion. Before ANGII infusion, both EC-Del1 and WT littermates had similar SBP (Figure 4A). After one week of ANGII-infusion, SBP was increased (P<0.01) similarly both in WT and EC-Del1 mice compared to vehicle-infused mice (Figure 4A). In the following weeks, SBP increased gradually in WT, but not in EC-Del1 mice, resulting in profound differences in SBP among the groups at weeks 2 (P<0.05), 3 (P<0.01) and 4 (P<0.01). Endothelial function was tested with assessment of ACh-mediated endothelium-dependent aortic relaxation. ACh-mediated maximal aortic relaxation after ANGII infusion was 62% in WT and 81% in EC-Del1 mice (P<0.01, Figure 4B). Vehicle-infused EC-Del1 and WT mice showed similar, approximately 90%, ACh-mediated aortic relaxation. Maximum SNP-mediated endothelium-independent relaxation was not different between groups (Figure 4C). We also assessed aortic stiffness by evaluating diameter-tension relationship in isolated aorta in a passive state. By gradual increase in diameter, wall tension increased in all groups (Figure 4D). However, the wall tension was significantly lower in ANGII-infused EC-Del1 mice compared to WT controls (P<0.05, Figure 4D).

DEL-1 overexpression suppresses inflammation in aorta and heart

Studies have shown that ANGII-infusion promotes T-cell inflammation and IL-17 mediated aortic and cardiac remodeling, along with progression of hypertension (6–12). We therefore investigated whether the protective effects of DEL-1 on ANGII-induced cardiovascular remodeling and development of hypertension is associated with DEL-1-mediated inhibition of IL-17-dependent inflammation. To this end, we assessed the numbers of CD45+ leukocytes, TCRβ+ T-cells and CD45+IL17+ leukocytes in aorta and heart. Compared to vehicle, ANGII-infusion profoundly increased CD45+ leukocytes, TCRβ+ T-cells and CD45+IL17+ leukocytes in aortas and hearts of WT mice (P<0.01, Figure 4E-L). Aortas and hearts of EC-Del1 mice had significantly less CD45+ leukocytes, TCRβ+ T-cells and CD45+IL17+ leukocytes after ANGII-infusion compared to WT controls (P<0.01, Figure 4E-L).

DEL-1 overexpression inhibits activation of MMP2 in aorta and heart

Besides inflammation, increased levels of MMP2 critically contribute to aortic and cardiac remodeling in hypertension (23, 24). Based on this, we tested MMP2 activity in aorta and heart.

ANGII-infused WT mice showed a ~6-fold increase in latent pro-MMP2 and ~8-fold increase in active MMP2 in aorta compared to vehicle-infused WT mice (P<0.01, Figure 5A, B). ANGII-infused EC-Del1 mice showed similar increase in latent pro-MMP2, but did not show the increase in active MMP2 compared to WT mice (Figure 5A, B). In hearts, ANGII-infused WT mice demonstrated a ~4-fold increase in latent pro-MMP2 and a ~3-fold increase in active MMP2 (P<0.01), whereas EC-Del1 mice showed a similar increase in latent pro-MMP2, but no increase in active MMP2 (Figure 5A, C).

DEL-1 overexpression protects form ANGII-induced increase in pro-fibrotic and pro-inflammatory profiles in aorta and heart

In addition to assessment of fibrosis and inflammation in aorta and heart using histology, we quantified mRNA levels for multiple pro-fibrotic markers in these organs. These markers are presented in the Supplemental Figure 1A-P (aorta) and 2A-O (heart). Pro-fibrotic markers in aorta such as collagen 1, 3 and fibronectin were increased in ANGII-infused WT mice compared to vehicle (P<0.01, Supplemental Figure 1A-C). In heart, both the pro-fibrotic markers and markers of hypertrophy such as Myh-7, mBNP, actin were increased and Serca decreased (P<0.01, Supplemental Figure 2A-F). ANGII-infused EC-Del1 mice showed less mRNA levels of aortic collagen 1, 3 and fibronectin compared to WT controls (P<0.01, Supplemental Figure 1A-C). In heart, these mice also had less mRNA levels of Myh-7, mBNP and actin, along with more Serca (P<0.01, Supplemental Figure 2A-F). Furthermore, mRNA and/or protein levels of pro-inflammatory factors (IL-17, IL-6, ICAM1, VCAM1, TGF-β1, INF-γ, TNF-α) were assessed and found to be increased in ANGII-infused WT mice compared to vehicle both in aorta (P<0.01, Supplemental Figure 1E-N) and heart (P<0.01, Supplemental Figure 2G-M). ANGII-infused EC-Del1 mice, however, showed lower mRNA and protein levels of these pro-inflammatory factors both in aorta (P<0.01, Supplemental Figure 1E-N) and heart (P<0.01, Supplemental Figure 2G-M). Assessment of anti-inflammatory IL-10 revealed that ANGII-infused EC-Del1 mice had higher levels of IL-10 than WT controls both in aorta (P<0.05, Supplemental Figure 1O) and heart (P<0.01, Supplemental Figure 2N). We also quantified mRNA levels of DEL-1, which was 3 to 4 times higher in heart (P<0.01, Supplemental Figure 1P) and aorta (P<0.01, Supplemental Figure 2O) of EC-Del1 mice, respectively. ANGII-infusion did not change mRNA levels of DEL-1.

Recombinant DEL-1 prevents cardiovascular organ damage when injected before established hypertension

In the prevention study we tested efficacy of DEL-1 in protection from ANGII-induced cardiovascular damage. For this, recombinant DEL-1-Fc or Fc protein as a control was first injected in WT mice two days before ANGII-infusion and then every other day during 2-weeks of the infusion with ANGII or vehicle (Figure 6). Fc-treated mice infused with ANGII demonstrated aortic remodeling with higher adventitial collagen (P<0.01, Figure 6A, D), medial thickness (P<0.01, Figure 5B, E) and decrease in elastin area (P<0.01, Figure 6C, F) compared to vehicle-infused mice. Compared to Fc-treated mice, DEL-1-Fc treatment completely protected from the effects of ANGII, resulting in lower adventitial collagen (P<0.01, Figure 6A, D) and medial thickness (P<0.05, Figure 6B, E), along with higher elastin area (P<0.01, Figure 6C, F). Fc-treated mice infused with ANGII also developed cardiac remodeling with decrease in LV lumen-to-wall ratio (P<0.01, Figure 6G, K), increased LV cardiomyocyte cross-sectional area (P<0.01, Figure 6H, L) and interstitial (P<0.01, Figure 6I, M) and perivascular coronary fibrosis (P<0.01, Figure 6J, N). Treatment of ANGII-infused mice with DEL-1-Fc, but not with Fc control, protected from cardiac remodeling, resulting in a higher LV lumen-to-wall ratio (P<0.01, Figure 6G, K) and a lower cardiomyocyte cross-sectional area (P<0.05, Figure 6H, L), as well as less interstitial (P<0.01, Figure 6I, M) and perivascular collagen (P<0.01, Figure 6J, N).

After 2-weeks of ANGII infusion, DEL-1-Fc treated mice had a lower (P<0.05) SBP compared to mice treated with Fc (P<0.05, Figure 7A). However, SBP did not differ in mice before or at the first week of ANGII infusion. ACh-mediated endothelium-dependent maximal aortic relaxation was ~70% in ANGII-infused Fc-treated mice and ~85% in mice treated with DEL-1-Fc (P<0.05, Figure 7B). There was no difference in maximum SNP-mediated endothelium-independent relaxation (Figure 7C). Assessment of diameter-tension relationship in isolated aorta in a passive state showed, that wall tension increased in all groups by gradually increasing the diameter (Figure 7D). However, the wall tension was lower in ANGII-infused DEL-1-Fc treated mice compared to mice treated with Fc alone (P<0.05, Figure 7D).

Fc-treated mice showed profound increases in CD45+ leukocytes, TCRβ+ T-cells and CD45+IL17+ leukocytes in aorta and heart after ANGII-infusion, compared to vehicle-infused Fc-treated control mice (P<0.01, Figure 7E-L). DEL-1-Fc treated mice showed significantly lower counts of CD45+ leukocytes, TCRβ+ T-cells and CD45+IL17+ leukocytes (P<0.05, Figure 7E-L) in aorta and heart after ANGII infusion compared to Fc-treated control mice.

Assessment of latent and active MMP2 showed, that Fc-treated mice had increased pro- and active MMP2 levels in aorta (P<0.01, Figure 8A, B) and heart (P<0.01, Figure 8A, C) after ANGII

infusion. Mice treated with DEL-1-Fc showed similar increase in latent pro-MMP2, but less active MMP2 in aorta (P<0.01, Figure 8A, B) and heart (P<0.01, Figure 8A, C). ANGII infusion increased mRNA levels of aortic pro-fibrotic markers, such as collagen 1, 3 and fibronectin in Fc-treated mice (P<0.01, Supplemental Figure 3A-C), whereas these levels were lower in DEL-1-Fc treated mice (P<0.01, Supplemental Figure 3A-C). In heart, mRNA levels of pro-fibrotic and hypertrophy markers, such as collagen 1, 3, Myh-7, mBNP, actin were increased and Serca decreased in Fc-, but not in DEL-1-Fc treated mice (P<0.01, Supplemental Figure 3A-F). We furthermore assessed mRNA and protein levels of pro-inflammatory factors (IL-17, IL-6, ICAM1, VCAM1, TGF-β1, INF-γ, TNF-α), which were increased in Fc treated mice after ANGII-infusion compared to DEL-1-Fc treated mice both in aorta (P<0.01, Supplemental Figure 2D-L) and heart (P<0.01, Supplemental Figure 4G-K). Levels of anti-inflammatory IL-10 were higher in ANGII-infused DEL-1-Fc treated mice compared to Fc treatment in aorta (P<0.05, Figure 3M) and heart (P<0.01, Figure 4L).

Therapeutic intervention with recombinant DEL-1 after ANGII-induced established hypertension protects from cardiovascular organ damage via αvβ3-integrin-dependent mechanisms

In the second interventional study, we tested efficacy of DEL-1 in abrogation of ANGII-induced cardiovascular damage after established hypertension and investigated its mechanisms of action. For this, WT mice were infused with ANGII for six days before treatment with injections of either recombinant DEL-1-Fc, Fc protein as a control or mutant DEL-1-RGE-Fc, which does not bind to αvβ3-integrin, started. While ANGII infusion continued treatments were undertaken every day up to day 12th of ANGII infusion (Figure 8). We compared the effects of mice treated with Fc alone to those treated with DEL-1-Fc or DEL-1-RGE-Fc. Compared to vehicle, Fc treated mice infused with ANGII developed aortic remodeling with increased adventitial collagen (P<0.01, Figure 9A, D), increased medial thickness (P<0.01, Figure 9B, E) and decreased elastin (P<0.01, Figure 9C, F). Compared with Fc-treated mice, DEL-1-Fc treatment resulted in less adventitial collagen (P<0.01, Figure 9A, D) and medial thickness (P<0.05, Figure 9B, E) and more elastin content (P<0.01, Figure 9C, F), whereas aortas of De-1-RGE-Fc treated mice did not differ from those treated with Fc alone. Fc treated mice infused with ANGII also developed cardiac remodeling with decrease in LV lumen-to-wall ratio (P<0.01, Figure 9G, K), increased LV cardiomyocyte cross-sectional area (P<0.01, Figure 9H, L) and interstitial (P<0.01, Figure 9I, M) and perivascular coronary fibrosis (P<0.01, Figure 9J, N). Treatment with DEL-1-Fc, but not with DEL-1-RGE-Fc resulted in a higher LV lumen-to-wall ratio (P<0.01, Figure 9G, K) and a lower cardiomyocyte cross-sectional area (P<0.05, Figure 9H, L), as well as less interstitial (P<0.01, Figure 9I, M) and perivascular collagen (P<0.01, Figure 9J, N).

Assessment of SBP showed, that DEL-1-Fc treated mice had a lower (P<0.01) SBP compared to those treated with DEL-1-RGE-Fc or Fc (P<0.05, Figure 10A) at the 2nd week of ANGII infusion. However, SBP did not differ in mice before or at the 6th day of ANGII infusion when the injections started. At the end of treatment periods, ACh-mediated endothelium-dependent maximal aortic relaxation was ~83% in DEL-1-Fc treated mice and ~72% and ~68% in DEL-1-RGE-Fc or Fc-treated mice, respectively (P<0.05, Figure 10B). There was no difference in maximum SNP-mediated endothelium-independent relaxations between groups (Figure 10C). Assessment of diameter-tension relationship in isolated aorta showed, that all groups responded with increase in wall tension by gradually increasing the diameter (Figure 10D). However, the wall tension was lower in ANGII-infused DEL-1-Fc treated mice compared to DEL-1-RGE-Fc- or Fc-treated control mice (P<0.05, Figure 10D).

ANGII-infused Fc-treated mice showed increases in CD45+ leukocytes, TCRβ+ T-cells and CD45+IL17+ leukocytes, along with decrease in CD25+FoxP3+ Tregs in aorta and heart compared to vehicle-infused Fc-treated mice (P<0.01, Figure 10E-N). DEL-1-Fc treated mice infused with ANGII showed significantly lower counts of CD45+ leukocytes, TCRβ+ T-cells and CD45+IL17+ leukocytes, along with higher numbers of in CD25+FoxP3+ Tregs in aorta and heart compared to DEL-1-RGE-Fc or Fc-treated mice (P<0.01, Figure 10E-N). We further assessed the levels of latent and active MMP2 after ANGII infusion, which showed that Fc-treated mice had increased latent pro- and active MMP2 in aorta (P<0.01, Figure 11A, B) and heart (P<0.01, Figure 11A, C). Increase in latent pro-MMP2 was not different in mice treated with DEL-1-Fc, DEL-1-RGE-Fc or Fc alone, whereas active MMP2 was lower in DEL-1-Fc than in DEL-1-RGE-Fc or Fc treated mice both in aorta (P<0.01, Figure 11A, B) and heart (P<0.01, Figure 11A, C). mRNA levels of aortic pro-fibrotic markers, such as collagen 1, 3 and fibronectin were also less in DEL-1-Fc than DEL-1-RGE-Fc or Fc treated mice (P<0.01, Supplemental Figure 5A-C). Cardiac mRNA levels of pro-fibrotic and hypertrophy markers, such as collagen 1, 3, Myh-7, mBNP, actin were decreased and Serca increased in DEL-1-Fc compared to DEL-1-RGE-Fc or Fc treated mice (P<0.01, Supplemental Figure 6A-F). We further assessed mRNA and/or protein levels of pro-inflammatory factors (IL-17, IL-6, ICAM1, VCAM1, TGF-β1, INF-γ, TNF-α) and results showed that they were lower in DEL-1-Fc than DEL-1-RGE-Fc or Fc treated mice both in aorta (P<0.01, Supplemental Figure 5D-K) and heart (P<0.01, Supplemental Figure 6G-K). Levels of IL-10 were higher in ANGII-infused DEL-1-Fc treated mice compared to DEL-1-RGE-Fc or Fc treatment in aorta (P<0.05, Supplemental Figure 5L) and heart (P<0.01, Figure 6L).

Therapeutic intervention with recombinant DEL-1 after DOCA-salt-induced established hypertension protects from cardiovascular organ damage

Effects of DEL-1 was tested in another model of hypertension induced with DOCA-salt. In this third therapeutic study, injections started at the 10th day with the last injection at the 18th day of 21-days of DOCA-salt hypertension. Histological assessments showed that DEL-1-Fc treated mice had profoundly less aortic adventitial collagen (P<0.01, Figure 12A, D) and medial thickening (P<0.05, Figure 12B, E), with more elastin (P<0.01, Figure 12C, F) compared to Fc-treated mice. Assessment of cardiac parameters demonstrated that DEL-1-Fc treated mice had higher LV lumen-to-wall ratio (P<0.01, Figure 12G, J), less cardiomyocyte cross-sectional area (P<0.05, Figure 12H, K) and interstitial collagen (P<0.01, Figure 12I, L) compared to mice treated with Fc. Treatments with DEL-1-RGE-Fc did not affect aortic or cardiac remodeling and showed no difference from those treated with Fc (Figure 12A-L). Number of CD45+, CD45+TCRβ+, CD45+TCRβ+CD4+, CD45+TCRβ+CD8+ and CD4+IL-17A+ cells in aorta (Figure 13A-E) and heart (Figure 13G-K) was lower in DEL-1-Fc treated mice compared to mice treated with Fc alone. Treatments with DEL-1-Fc resulted in increased numbers of CD4+CD25+FoxP3+ Tregs compared to Fc treatment both in aorta (Figure 13F) and heart (Figure 13L). Injections of DEL-1-RGE-Fc did not affect numbers of inflammatory cells in aorta and heart and showed no difference from those mice treated with Fc (Figure 13A-L). Systolic blood pressure did not differ in mice before injections on the 7th day of DOCA-salt hypertension (Figure 13N). After injection of DEL-1-Fc, SBP did not further increase in this group, whereas gradual increase in SBP was observed in DEL-1-RGE-Fc and Fc treated groups. This resulted in ~10 mm Hg lower SBP in DEL-1-FC injected mice compared to mice treated with Fc or DEL-1-RGE-Fc on the day 14 and 21. Mice implanted with placebo pallet and treated with Fc remained normotensive.

DEL-1 inhibits αvβ3-integrin-dependent activation of latent pro-MMP2 in vascular tissue

In several consecutive ex-vivo experiments, we studied the role and mechanism of DEL-1 in inhibition of activation of latent pro-MMP2 in aorta and cultured human aortic smooth muscle cells (Figure 14). These cells were chosen because SMCs are the major source of MMP2 in aorta and αvβ3 integrin on SMCs is critical in activation of latent pro-MMP2 (22, 25). In the first set of experiments, aortas were isolated from WT and EC-Del1 mice followed by stimulation with ANGII/ET1 and assessment of latent pro- and active MMP2 (Figure 114A). Compared to vehicle, ANGII/ET1 stimulation increased latent pro-MMP2 in isolated aortas of both WT and EC-Del1 mice similarly (P<0.01, Figure 14A), whereas active MMP2 was less in aortas of EC-Del1 mice (P<0.01, Figure 14A). Because we employed endothelial specific EC-Del1 mice, in the second set of

experiments, we stimulated isolated aortas from WT and EC-Del1 mice after removal of endothelium (Figure 14B). Stimulation with ANGII/ET1 similarly increased both latent pro- and active MMP2 in isolated aortas of WT and EC-Del1 mice in the absence of endothelium (P<0.01, Figure 14B) showing no difference in MMP2 in aortas of mice. In the third set of experiments, isolated aortas of WT mice were pre-treated with plasmas of EC-Del1 or WT mice followed by stimulation with ANGII/ET1. Isolated aortas pre-treated with plasma from EC-Del1 mice showed less active MMP2 than aortas pre-treated with plasmas from WT mice (P<0.01, Figure 14C). Treatment with plasma from EC-Del1 mice did not affect increase in latent pro-MMP2 (Figure 14C). In the fourth set of experiments, we studied the role of αvβ3-integrin in DEL-1 mediated inhibition of activation of latent pro-MMP2 by pre-treating isolated aortas of WT mice with Fc, DEL-1 Fc or DEL-1-RGE-Fc and then stimulating with ANGII/ET1. Stimulation with ANGII/ET1 increased latent pro-MMP2 equally in isolated aortas treated with Fc, DEL-1 Fc or DEL-1-RGE-Fc (P<0.01, Figure 14D). However, active MMP2 was less in DEL-1-Fc-treated aorta, but not in aorta treated with DEL-1-RGE-Fc (P<0.01, Figure 14D). In the fifth set of experiments, we studied the effects of treatment with plasmas from WT mice injected with Fc, DEL-1-Fc or DEL-1-RGE-Fc on inhibition of activation of latent pro-MMP2 in cultured human aortic smooth muscle cells (Figure 14E). Treatment with plasma from Fc injected mice did not inhibit ANGII/ET1 mediated increase in latent pro- and active MMP2. Treatment with plasmas from EC-Del1 mice did not affect latent pro-MMP2 but decreased active MMP2 (P<0.01, Figure 14E). Plasmas from DEL-1-Fc, but not DEL-1-RGE-Fc injected mice decreased active MMP2 without affecting latent pro-MMP2 (P<0.01). In the final set of experiments, cultured human aortic smooth muscle cells were pre-treated with recombinant DEL-1-Fc or DEL-1-RGE-Fc, along with the pharmacological inhibitor of αvβ3-integrin cilengitide followed by stimulation with ANGII/ET1 (Figure 14F). Treatment with DEL-1-Fc or cilengitide decreased ANGII/ET1-induced active MMP2 without affecting latent pro-MMP2 (P<0.01), whereas treatment with DEL-1-RGE-Fc or Fc did not affect the induction of active MMP2, thus conclusively implicating αvβ3-integrin as the target of DEL-1.

DEL-1 inhibits αvβ3-integrin-dependent activation of latent pro-MMP2 in human isolated aorta

Pieces of human isolated aorta were pretreated with plasmas from Fc, DEL-1-Fc, DEL-1-RGE-Fc injected WT mice or with plasma from EC-Del1 mice (Figure 15A, B). After pretreatment, aortas were stimulated with ANGII/ET1 or vehicle. In-situ zymography on human isolated aorta showed that compared to vehicle, ANGII/ET1 increased gelatinolytic activity of MMP2 in aortic sections pretreated with plasma from Fc-treated mice (Figure 15C, D). Pretreatment with plasmas from EC-Del1 or DEL-1-Fc-treated mice resulted in inhibition of the gelatinolytic activity, whereas

pretreatment with plasma from DEL-1-RGE-Fc-treated mice did not inhibit the gelatinolytic activity. Control pretreatment with EDTA resulted in complete inhibition of gelatinolytic activity of zinc dependent MMP2.

Additionally, MMP2 was extracted from aortas and its in vitro activity was assessed. The results were similar to those of the in-situ zymography. Compared to vehicle, MMP2 activity was higher in aortic sections pretreated with plasmas from Fc-injected mice and stimulated with ANGII/ET1 (Figure 15E). Pretreatment with plasmas from EC-Del1 or DEL-1-Fc-treated mice, but not from DEL-1-RGE-Fc-treated mice resulted in inhibition of MMP2 activity. We further assessed components of activation machinery of pro-MMP2, such as furin and MT1-MMP, which in conjunction with αvβ3-integrin activate latent pro-MMP2 (25, 26). Treatment with various plasmas (from EC-Del1 mice or DEL-1-Fc-, DEL-1-RGE-Fc- or Fc-treated mice) did not inhibit furin or MT1-MMP in human isolated aorta (Figure 15F, G).

Discussion

We demonstrate a novel protective function of DEL-1 in two models of hypertension-induced cardiovascular remodeling. Consistent findings from EC-Del1 mice with endothelial-specific DEL-1 overexpression and therapeutic intervention studies with injections of recombinant DEL-1 provide compelling evidence that DEL-1 protects from adverse remodeling both in aorta and heart, as well as hinders the progression of hypertension. We propose that the mechanisms of action of DEL-1 largely depend on αvβ3-integrin-dependent effects. By interacting with the αvβ3-integrin, DEL-1 inhibits activation of latent pro-MMP2 and stabilizes anti-inflammatory Treg/IL-10 response with consequent suppression of IL-17 production and pro-inflammatory cell recruitment in target organs.

Cardiovascular remodeling is a hallmark of hypertension. Vascular and cardiac remodeling interact in a complex manner, which augment each other leading to further augmentation of SBP and organ damage (2, 3). Therefore, control of arterial pressure and attenuation of cardiovascular remodeling by therapeutic intervention is of critical importance. We demonstrate that DEL-1 can prevent the hypertension-induced aortic and cardiac remodeling, as well as it can abrogate further progression of systolic blood pressure. This is supported by results obtained from four different sets of animal experiments using genetic overexpression of endothelial DEL-1 and therapeutic injections of recombinant DEL-1-Fc before or after onset of hypertension. Findings from EC-Del-1 model and the 1st therapeutic study demonstrate that DEL-1 abrogates progression of hypertension. Whereas SBP was similar in EC-Del1 or DEL-1-Fc treated mice to their respective controls in the first week of hypertension induction, SBP did not further increase in EC-Del1 or DEL-1-Fc treated mice at later times. Initial increase in SBP in the 1st week is merely a result of the vasoconstrictive effect in both models resulting in an increase in LV afterload (7, 10, 11). Further progression of SBP seen from 2nd week of induction of hypertension can be attributed to aortic remodeling/stiffening and worsening of endothelial function, important parameters, which augment systolic hypertension (5, 11). Stiffness of aorta reduces its capacity to expand (Windkessel effect) during systole, decrease LV afterload and damp the systolic pressure. Endothelial dysfunction causes decrease in bioavailability of NO, which may increase peripheral vessel tone. Therefore, arterial stiffening and endothelial dysfunction result in worsening of Windkessel function and increase in peripheral resistance, which ultimately drive the progression of SBP. Aortas of EC-Del1 or DEL-1-Fc treated mice were less stiff compared to their respective controls. This is demonstrated by assessment of aortic diameter-tension relationship, a parameter to assess vessel stiffness (38), which showed that aortas of EC-Del1 or DEL-1-Fc treated mice developed less passive tension compared to controls. These mice also had less aortic adventitial

fibrosis and medial thickening along with more elastin and profoundly improved endothelial function, which are additional indications that these mice had more elastic vessels with better endothelial function than their respective controls. Based on this, we conclude that DEL-1 did not interfere with vasoconstrictive effects and hence was unable to prevent the increase in SBP during the 1st week of hypertension induction. However, because DEL-1 prevented aortic remodeling/stiffness and endothelial dysfunction, it abrogated progression of SBP after the first up to the fourth week of hypertension.

Along with arterial remodeling, hypertension is a major risk factor for development of cardiac remodeling, resulting in concentric hypertrophic cardiomyopathy with coronary microvascular dysfunction accompanied with metabolic adaptations. If untreated, these pathological changes may lead to cardiac failure (3–5). Here, we demonstrate that DEL-1 also protects from cardiac remodeling. This is supported by echocardiographic findings showing, that compared to their WT controls, EC-Del1 mice have higher LV diameter and end-diastolic volume, as well as better systolic function showed by higher stroke volume. Histological assessment showed that EC-Del1 or Ec-DEL-1-Fc treated mice had higher LV lumen-to-wall ratio, with less cardiomyocyte cross-sectional area, along with less interstitial and coronary fibrosis. EC-Del1 mice also showed better coronary perfusion by demonstrating improved coronary flow responses to adenosine and reactive hyperemia compared to WT littermates. It is notable that after ANGII-infusion, WT mice had extremely worsened response to adenosine, which was accompanied with a severe decrease in mRNA levels of adenosine receptors type A2A and A2B. These receptors are major mediators of coronary vasodilation in response to adenosine (39). These findings are consistent with previous studies showing that ANGII worsens adenosine-induced vasodilation by diminishing adenosine receptor expression (39). However, it is not fully understood how ANGII reduces adenosine receptor expression. Because EC-Del1 mice showed better responses to adenosine and higher A2A and A2B receptor expression, anti-inflammatory effects of DEL-1 might have at least partly contributed to higher expressions of these receptors. Nevertheless, the better coronary response to adenosine in EC-Del1 mice can be explained by higher expression of adenosine receptors, especially type A2A and A2B. Worsened coronary dilatation to adenosine and flow stop, besides diminished expression of adenosine receptors can be a result of cardiac and coronary vessel remodeling. Increase in cardiomyocyte cross sectional area and deposition of collagen in the extracellular matrix exerts increased extravascular pressure limiting the expansion of vessel radius and therefore limiting its dilatation. Moreover, perivascular fibrosis seen after ANGII-infusion can stiffen coronary vessels and further hinder its dilatory capacity. This is especially evident in coronary dilatation after flow stop, because the dilatation is not mediated only via

adenosine and its receptors but is a result of several mechanisms including metabolic, endothelial NO and myogenic responses. Therefore, better dilatory response of coronary vessels to adenosine and specially to flow stop in ANGII-infused EC-Del1 mice can be attributed both to higher expression of adenosine receptors as well as blunted cardiac and coronary vessel remodeling. Worsened coronary perfusion during cardiac hypertrophy leads to myocardial hypoxia and forces cardiomyocyte metabolic adaptation by switching to increased glucose metabolism (4). This was evidenced in ANGII-infused WT mice which showed higher lactate and malate levels in effluents of perfused hearts, whereas EC-Del1 mice had lower levels of these metabolites. These findings clearly demonstrate that DEL-1 improved cardiac parameters with improved coronary perfusion and blunted the increased reliance on glucose metabolism. Altogether, the findings in EC-Del1 mice and in therapeutic studies clearly demonstrate, that DEL-1 attenuates hypertension-induced cardiovascular remodeling and further progression of SBP.

In this study, we also provide mechanistic proof of the actions of DEL-1 in ANGII-induced hypertension and cardiovascular remodeling. We reveal a novel action of DEL-1, a potent inhibitory effect of αvβ3-integrin-dependent activation of latent MMP2. Studies in EC-Del1 mice and therapeutic studies clearly demonstrate low levels of active MMP2 in aortas and hearts, without differences in latent pro-MMP2 levels after ANGII-infusions. This suggests that DEL-1 did not affect expression of latent pro-MMP2, but inhibited αvβ3-integrin-dependent activation of latent pro-MMP2 to active MMP-2. The activation of latent pro-MMP2 is strictly regulated and hardly catalyzed by regular proteases. The activation rather depends on membrane αvβ3-integrin, which localizes pro-MMP2 at the cell membrane and facilitates its catalytic cleavage by membrane protease MT1-MMP (25, 26). Because, DEL-1 can bind to αvβ3-integrin through its RDG motif (30), we propose that binding of DEL-1 to αvβ3-integrin prevented this integrin-dependent activation of latent pro-MMP2. This is supported by three experimental setups using mice and human material, which demonstrate that unlike DEL-1-Fc, mutant DEL-1-RGE-Fc, which does not interact with the αvβ3-integrin, was unable to inhibit activation of latent pro-MMP2. Notably, a pharmacological inhibitor of αvβ3-integrin acted like DEL-1-Fc and lowered active MMP2 levels without affecting pro-MMP2 levels. With this, we demonstrate for the first time that DEL-1 can inhibit the activation of latent pro-MMP2 by blocking αvβ3-integrin/pro-MMP2 interaction and inhibit its catalytic activation. We propose that the inhibitory effect of DEL-1 on activation of latent pro-MMP2 is an important mechanism of action of DEL-1 in prevention of ANGII-induced cardiovascular remodeling, because MMP2 is critically involved in hypertensive aortic and cardiac remodeling (23, 24). MMP2 is capable of degrading elastic fibers in aorta leading to enhanced stiffening, whereas it also contributes to aortic remodeling by increasing endothelial permeability

and promoting endothelial dysfunction, which may facilitate vascular inflammation (22, 40). Furthermore, a recent study where authors used mice lacking MMP2 clearly demonstrates that these mice are protected from ANGII-induced aortic remodeling (23). Mice lacking MMP2 also showed less aortic monocyte/macrophage and T cell infiltration, along with better endothelial function and decreased aortic stiffness. Importantly, these protective effects were observed in a mouse model lacking MMP2 in vascular cells. Furthermore, Diaz-Canestro et. al. demonstrate that MMP2 knockdown by siRNA protected mice from age-dependent carotid stiffening and an increased elastin-to-collagen-ratio, which was associated with increased eNOS phosphorylation and higher levels of cGMP (24). Therefore, inhibition of MMP2 by DEL-1 in aorta may represent an important mechanism of action in protection from at least vascular remodeling during hypertension. Although mice lacking MMP2 show protection from vascular stiffening, they still demonstrate cardiac inflammation and remodeling (23). DEL-1, however, was able to inhibit both cardiac and aortic inflammation and prevent cardiovascular remodeling. Based on this, we propose that along with inhibition of pro-MMP2 activation, direct anti-inflammatory effects of DEL-1 may extend protection from cardiac remodeling.

It has been established that inflammation is a critical driving force in hypertension-induced cardiovascular remodeling and progression of hypertension (6–13). There are two major proinflammatory actions driving hypertensive cardiovascular remodeling and hypertension: leukocyte recruitment into cardiovascular tissues followed by T-cell/IL-17-driven inflammation and simultaneously a destabilized/reduced anti-inflammatory CD4+FoxP3+ Treg/IL-10 response (6–12, 15–17). Genetic anti-inflammatory approaches such as depletion of T-cells in RAG1 KO mice or adoptive transfer of Tregs, along with substitution of IL-10 were shown to protect from ANGII-induced cardiovascular remodeling (6–12, 15–17). Previously, we showed that DEL-1 exerts its potent anti-inflammatory actions via three major mechanisms: it inhibits β2-integrin-dependent recruitment of leukocytes and promotes resolution of inflammation via αvβ3-integrin-dependent macrophage efferocytosis and induction of anti-inflammatory Treg response (35, 36). Here, we demonstrate that in all our four mouse experimental models, EC-Del1 or DEL-1-Fc, but not mutant DEL-1-RGE-Fc treated mice were protected from hypertension-induced cardiovascular inflammation by showing less CD45+ leukocytes, TCRβ+ and CD45+IL-17+ leukocytes in aorta and heart. Moreover, DEL-1-Fc injections during hypertension resulted in higher numbers of CD25+/FoxP3+ Treg cells and more IL-10 compared to injections of DEL-1-RGE-Fc. The latter finding is consistent with our previous report demonstrating that DEL-1 induced a Treg response via αvβ3/RUNX1/FoxP3 mechanistic pathway (35). Finally, as described above, only injection of DEL-1-Fc and not DEL-1-RGE-Fc was able to abrogate cardiovascular remodeling and

progression of hypertension. This indicates that anti-inflammatory actions of DEL-1 and protection from cardiovascular remodeling were αvβ3-integrin-dependent. Therefore, αvβ3-integrin-dependent actions, such as stabilization of the Treg/IL-10 response and inhibition of pro-MMP2 activation are of critical importance. This might be true, because hypertension-induced cardiovascular inflammation and organ damage is associated with loss of Treg/IL-10 responses and overactivation enhanced activation of MMP2 (13, 15, 17, 18, 23, 41). We want to point out that although mutant DEL-1-RGE-Fc is unable to mediate αvβ3-integrin-dependent actions of DEL-1, it is still able to bind to β2-integrins and might be able to inhibit recruitment of leukocytes (33). However, DEL-1-RGE-Fc was unable to suppress cardiovascular inflammation and organ damage. This indicates that the direct inhibition of leukocyte recruitment alone is most likely not sufficient to secure overall effective anti-inflammatory actions of DEL-1 and protect from cardiovascular remodeling. Therefore, we propose that the actions of DEL-1, which are mediated by interaction with αvβ3-integrin, ensure the efficient anti-inflammatory actions and protection from hypertensive cardiovascular remodeling and progression of hypertension.

Efferocytosis is another αvβ3-integrin-dependent inflammation resolving action of DEL-1 (36). Although DEL-1-mediated efferocytosis was not addressed in our hypertension models, it is unlikely that this action is relevant at least in our EC-Del1 model. Previously we showed that DEL-1-dependent promotion of efferocytosis and resolution of inflammation depends on cell-specific expression of DEL-1 in model of periodontitis. While endothelial overexpression of DEL-1, the model employed here, does not promote efferocytosis, macrophage specific expression of DEL-1 resolves inflammation by efferocytosis (36). However, we cannot rule out the contribution of efferocytosis in therapeutic studies because injection of DEL-1-Fc is a different mode of intervention than overexpression of DEL-1 and it might have, at least partly, acted via efferocytosis. Based on this, we propose that in the model of hypertension employed here, the major mechanisms of action of DEL-1 were mediated via αvβ3-integrin. These actions include inhibition of pro-MMP2 activation and stabilization of anti-inflammatory Treg/IL-10 response. These αvβ3-integrin-dependent actions led to suppression of inflammation and ameliorated remodeling in cardiovascular tissues, as well as blunted progression of hypertension. Whereas inhibition of pro-MMP2 activation might have been sufficient to protect from aortic remodeling and progression of hypertension, additional direct anti-inflammatory actions of DEL-1 were most likely critical to ensure protection from cardiac remodeling.

In conclusion, as summarized in Figure 15H, our findings provide compelling evidence that DEL-1 is a potent factor in attenuating ANGII- or DOCA-salt induced hypertensive aortic and cardiac remodeling and consequently progression of hypertension. In this context, DEL-1 may act via a

combination of mechanisms including, but not limited to, stabilization of Treg/IL10 responses and inhibition of activation of latent pro-MMP2, which were associated with decreased inflammatory cell recruitment. Given the potent effects seen after therapeutic application of DEL-1-Fc, we specifically propose that DEL-1 is an attractive potential therapeutic agent against hypertension-induced cardiovascular remodeling. These findings greatly widen the horizon of potent immunomodulating effects of DEL-1 in inflammation-driven diseases.

Methods

Mice - induction of hypertension and cardiovascular remodeling

We used DEL-1 transgenic mice (EC-Del1) with endothelial-specific overexpression of DEL-1 (31, 42, 43) and their wild type (WT) littermates. Hypertension and cardiovascular remodeling were induced by employing two models of hypertension, infusion of 1.5 mg/kg/day of angiotensin II (ANGII, Sigma) up to for 4-weeks using osmotic minipumps (Alzet®, model 1001) and implanting deoxycorticosterone acetate-salt pellet (50 mg DOCA + 1% salt in drinking water) up to three weeks. The pumps and the DOCA pellets were implanted subcutaneously at the age of 12-weeks under anesthesia with 2% Isoflurane. Control mice were infused with vehicle (NaCl) or implanted with placebo pellets to control effects of ANGII and DOCA, respectively. Mice were sacrificed under deep anesthesia with combination of 270 mg/kg Ketamine and 30 mg/kg Xylazine.

Therapeutic studies in mice

Therapeutic efficacy of DEL-1 in ANGII-induced (infused for 2-weeks) hypertension and cardiovascular remodeling was tested by retro-orbital injection of recombinant soluble DEL-1-Fc in 12-week-old WT mice. Thirty micrograms of DEL-1 fused with Fc receptor was administered per injection per mouse in the 1st therapeutic study, whereas 20 µg per injection in the 2nd and 3rd therapeutic studies. Recombinant DEL-1-Fc was produced as previously described (33). Along with DEL-1-Fc protein with RGD motive, by which it binds to αvβ3-integrin (30), a mutant form of the protein was used with altered RGE motive (referred throughout the text as DEL-1-RGE-Fc), which is unable to bind to αvβ3-integrin and affect its function (35, 36). Three therapeutic studies were performed, one preventive, starting with one injection before start of ANGII infusions and injecting every second day after starting the infusions (Figure 6). In this study, the last injection was done at the 12th day of ANGII-infusion. In two other therapeutic studies, interventions with injections started after established hypertension at the 6th or 10th day of ANGII pump or DOCA pellet implantation (after established hypertension, Figures 9 and 12), respectively, followed by injections up to 12th (ANGII) and 18th (DOCA) days. A total of seven (ANGII) or eight (DOCA) injections were performed. As control (placebo) groups, mice were injected with Fc.

Experiments on human isolated aorta

Human thoracic aorta was donated after surgical removal of aortic aneurysm. Aortic sections were stored in vessel protection solution Tiprotec® (F. Köhler Chemie, Bensheim, Germany), which preserves cell function of the vessel wall for at least 24-hours (44). Only the non-dilated part of resected aortic segments was prepared and used for experiments. As described in Figure 13, the segments were divided (in approx. 5 mm long sections) and placed in a 12-well plate containing supplemented Dulbecco's Modified Eagle's tissue Medium (ThermoFischer, USA). Some

segments were pretreated with plasmas (diluted in the medium) of mice injected either with Fc, DEL-1-Fc, DEL-1-RGE-Fc, as well as plasmas of EC-Del1 mice for 30 min followed by stimulation with 1 µmol/L ANGII/ET1 for 8 hours. After pretreatments and stimulations, aortic segments were collected for in-situ zymography and enzyme assays (described below).

In-situ zymography and MMP2/Furin/MT1MMP assays

In situ gelatin zymography was performed for assessment of gelatinolytic activity of MMP2 in 8 µM thick aortic tissue section fixed in zinc-based fixative (0.1 M Tris pH 7.4, 36.7 mM $ZnCl_2$, 27.3 mM $ZnAc_2$, 0.63 mM $CaAc_2$) and embedded in paraffin (45). After deparaffinization in xylene the tissue sections were rehydrated gradually in alcohol baths (100%, 3x2 min; 96% 2x2 min; 70% 2 min; 40% 2 min, H_2O 2 min). Fluorogenic MMP2 substrate (0.1 % DQ gelatin, D12054 ThermoFisher), which becomes fluorescent upon catalytic cleavage by MMP2, was added to the tissue sections and incubated in a dark humid chamber at 37°C for 20 h. The sections were then fixed in 4% neutral-buffered formalin for 10 min in the dark, followed by washing in PBS baths (2x5 min). Finally, the tissue sections were mounted with glycerol containing DAPI to counterstain the nuclei and imaged with fluorescent microscopy (ApoTome, Zeiss, Germany). Because MMP2 is a Zn-dependent enzyme, some sections were incubated with fluorogenic MMP2 substrate mixed with 1 mmol/L EDTA to control for specific MMP2 activity. Fluorogenic signal intensity as a value for MMP2 activity was quantified using ImageJ v1.52a. Furin activity in human aortic extracts was assessed using the fluorogenic substrate Pyr-Arg-Thr-Lys-Arg-AMC (MerckMillipore Corp, Massachusetts, USA) as previously described (26). A microplate reader (BMG Labtech©) was used to detect fluorescence at 365 nm excitation and 450 nm emission. Enzymatic activities of MMP2 and MT1-MMP in human aortic tissue extracts were quantified by specific enzyme assay kits (Abcam, ab139447 and ab 139454) according to the user manual.

Echocardiography

Echocardiography in mice was performed under anesthesia with 2% isoflurane using Fujifilm Visualsonics Vevo 3100 (with MX 400 transducer) echocardiography device. Obtained images were analyzed using Vevo Lab v2.1.0 software. Following parameters on the long axis of the left ventricle in B and M modes were analyzed: end-diastolic diameter and volume, end-systolic diameter and volume, end-diastolic and end-systolic ventricular wall thickness.

Isolated Langendorff heart experiments and metabolomics

Coronary vessel function was assessed on isolated hearts, which were perfused with Krebs-Henseleit perfusion buffer, as previously performed (46). The buffer was delivered through a cannula inserted in the ascending aorta, allowing perfusion of the coronary vessels by creating a retrograde flow in the aorta. Coronary flow reserve was then tested as reactive hyperemia (evoked

by stopping the flow for 20 s) or during infusion of 1 µmol/L adenosine. As perfusate drains as an effluent from the coronary circulation and drips from the apex of the heart, the effluent was collected and targeted metabolomics was performed employing LC-MS to assess metabolites of TCA cycle.

Histological stainings and morphometry

Remodeling of thoracic aorta was evaluated by assessment of adventitial collagen, elastin area and medial thickness employing sirius-red, elastica van Gieson and hematoxylin eosin stainings, respectively. Cardiovascular remodeling was evaluated by assessment of LV lumen-to-wall ratio and cardiomyocyte cross-sectional area after hematoxylin eosin staining, as well as interstitial and perivascular epicardial coronary collagen after sirius-red staining. Histological stainings and morphometry were performed as previously described (45).

Measurement of systolic blood pressure (SBP)

Before and after induction of hypertension SBP was measured weekly in conscious mice using the tail-cuff method with a BP recorder (UGO Basil) as performed previously (45). Mice were trained for the procedure for two weeks.

Assessment of endothelial function and aortic stiffness

Endothelial function was evaluated with assessment of acetylcholine (ACh)-mediated endothelium dependent aortic relaxation with Mulvany myograph (Power Lab/400, AD-Instruments, Spechbach, Germany) as previously performed (45). Along with ACh, sodium nitroprusside (SNP) was used to assess endothelium-independent aortic relaxation. Vessels were first pre-constricted with KCl (123.7 mmol/L) and then various concentrations of ACh and SNP were applied. Mulvany Myograph was also used to evaluate aortic stiffness by assessment of change in the passive diameter-tension relation as described previously (38).

Flow cytometry

Aorta with perivascular fat, as well as heart were digested by incubating tissues in Collagenase D, (1 mg/ml), Dispase II (1 mg/ml), DNAse I (0,1 mg/ml) in RPMI Medium. Tissues were cut into small pieces and vigorously shaken for 20 min at 37°C. After the passing via cell strainer (40 µm), the enzymatic reaction was blocked by PBS containing EDTA (2 mM), FBS (2%). After centrifugation, cells were resuspended in FACS buffer, stained with respective antibodies (CD45 eBioscience Clone 30F11 cat. 4277450, TCRβ Biolegend cat. 109222, CD4 MACS Miltenyi Biotec cat: 130-102-619, CD8 Methilenyi Biotec cat. 130-102-468, CD25 BD Pharmingen cat. 553075, FoxP3 eBioscience cat. 14-5773-82). For intracellular stainings, part of the cell suspension was used to culture cells in 24-well culture dishes in RPMI+10%FBS+1% Penicillin/Streptomycin

medium. After 24 hours, the cells were stimulated with PMA/Ionomycin containing brefeldin A and monensin (protein transport inhibitors) for four hours. To distinguish death cells Zombie Aqua Fixable viability kit (Biolegend) was used prior to antibody staining with anti-IL-17 antibody (ThermoFisher cat. 17-7177-81). The cells were assessed with flow cytometer (BD FACSCanto™ II Cell Analyzer). Data was analyzed with FlowJo software (Tree Star, Inc.).

Experiments on isolated mouse aorta and cultured human aortic smooth muscle cells

Thoracic aorta was isolated from 12-weeks old mice and placed in a 12-well plate containing supplemented Dulbecco's Modified Eagle's tissue Medium (ThermoFischer, USA). Primary cells were purchased from PromoCell® (Heidelberg, Germany). Cells were cultured on 12-well plate and stimulated with 1 µmol/L of ANGII and endothelin-1 (ET1, Sigma) for 8 hours to induce latent pro-MMP2 expression and activation. Effective concentrations of ANGII and ET1 were chosen based on our previous reports (26, 27). Various experiments on isolated aorta and human aortic SMCs were performed as described in Figure 11. The aorta and cells were pretreated with 0.1 µg/ml DEL-1-Fc or mutated DEL-1-RGE-Fc. As a control group, the cells were pre-treated with the pharmacological inhibitor of αvβ3 integrin cilengitide (1 µmol/L, Selleckchem). In other setup of experiments, the cells were pre-treated with plasmas of mice injected either with Fc, DEL-1-Fc, DEL-1-RGE-Fc plasma of EC-Del1 mice for 30 min. After this, plasma was removed and cells washed gently once followed by stimulation with 1 µmol/L ANGII/ET1 for 8 hours.

Gelatin zymography

The method was used to assess latent 72 kDa pro-MMP2 and 62 kDa active MMP2 in extracts of aorta and heart, as well as in SMC supernatant as previously performed (26, 27). Briefly, 0.25 % gelatin co-polymerized in 10 % polyacrylamide gel was used as a substrate for MMP2. Five microgram protein was separated with electrophoresis followed by incubation of gels in developing buffer. After 24 hours gels were stained with 0.1 % Coomassie blue. Latent pro-MMP2 and active MMP2 were detected as white bands on homogenously stained gel. Images were taken with PeqLab imager. Bands were quantified by densitometry using ImageJ v1.52a.

Reverse transcription qPCR and ELISA

Inflammatory and remodeling (hypertrophy, fibrosis) profiles in aorta and heart were evaluated by assessment of the mRNA or protein levels of various pro-inflammatory and remodeling markers. mRNA was isolated from homogenized tissues (Polytron, Elkhart, IN) using an mRNA isolation kit (RNeasy Plus Universal Mini Kit, Qiagen) according to the user manual. As previously described (44), one microgram of total mRNA was reverse transcribed using iScript cDNA Synthesis Kit (no. 170-8891; Bio-Rad) and cDNA was amplified using respective primers and SsoFast EvaGreen Supermix (no. 172-5240; Bio-Rad). Pro-inflammatory markers in tissue lysates were assessed

using V-Plex pro-inflammatory panel 1 mouse kit (K15048D-1, Mesoscale) according to the user manual.

Statistics

Results were analyzed with one- or, when appropriate, two-way ANOVA for multiple comparisons using GraphPad Prism version 6.01 for windows (GraphPad Software Inc, San Diego, CA, USA) followed by Bonferroni post hoc test to adjust for multiple comparisons. Data in Figures 4 A-D, 7 A-D, 10 A-D and 13N was analyzed for repeated measures. Data represent mean ± standard error of the mean (SEM). A *P* value less than 0.05 was considered significant.

Study approval

Experiments on human isolated aorta and animal studies were approved by the Ethics Committee of the University Hospital Dresden (approval EK26806201) and by institutional review board and Landesdirektion Sachsen (TVV 63-2015, TVV 37-2019), respectively.

Authors Contributions

Designing and supervising the work (I.K.), co-supervising the work (A.D., T.C.), conducting experiments (T.F., M.A., A.N., I.K., A.S., F.G., A.W., P.S., I.Kour. M.P), acquiring data (T.F., M.A., A.N., I.K., P.M. M.P.), analyzing data (T.F., M.A., A.N., I.K., A.D.,), interpreting data (I.K., A.D., V.T., T.C., G.H.) providing reagents (P.S., I.Kour., C.H., V.T., T.K., X.L., G.H., T.C.,), writing the manuscript (I.K., A.D.), editing the manuscript (G.H., T.C. V.T.).

Acknowledgements

We thank Birgit Zatschler, Carmen Friebel, Bettina Gercken, Sylvia Grossklaus for technical assistance. We also thank F. Köhler Chemie, Bensheim, Germany for providing Tiprotec®.

Sources of Funding

The work was supported by a research grant from German Research Foundation (Grant No.: KO 5833/1-1, TO 679/3-1, TO 679/5-1, HU 600/13-1), research training grant from the Else Kröner-Fresenius-Foundation (Grant No. 060_463519) and by NIH (grant DE026152). A.W. is recipient of a scholarship from the Carus Promotionskolleg Dresden (CPKD).

References

1. Day WH. A global brief on Hypertension World Health Day 2013. WHO 2013.
2. Kaess BM, et al. Aortic Stiffness, Blood Pressure Progression, and Incident Hypertension. *JAMA*. 2012;308(9):875.
3. Cooper LL, et al. Components of hemodynamic load and cardiovascular events: the Framingham Heart Study. *Circulation*. 2015;131(4):354-361
4. Kolwicz SC, Tian R. Glucose metabolism and cardiac hypertrophy. *Cardiovasc Res*. 2011;90(2):194-201.
5. Zoungas S, Asmar RP. Arterial Stiffness and Cardiovascular Therapy. *Clin Exp Pharmacol Physiol*. 2007;34:647-651.
6. Wu J, et al. Immune activation caused by vascular oxidation promotes fibrosis and hypertension. *J Clin Invest*. 2016;126(4):1607.
7. Kirabo A, et al. DC isoketal-modified proteins activate T cells and promote hypertension. *J Clin Invest*. 2014;124(10):4642-4656.
8. Wenzel P, et al. Lysozyme M-positive monocytes mediate angiotensin II-induced arterial hypertension and vascular dysfunction. *Circulation*. 2011;124(12):1370-1381.
9. Itani HA, et al. Activation of Human T Cells in hypertension: Studies of Humanized Mice and Hypertensive Humans. *Hypertension*. 2016;68(1):123-132.
10. Saleh MA, Norlander AE, Madhur MS. Inhibition of Interleukin-17A, But Not Interleukin-17F, Signaling Lowers Blood Pressure, and Reduces End-Organ Inflammation in Angiotensin II-Induced Hypertension. *JACC Basic Transl Sci*. 2016;1(7):606-616.
11. Madhur MS, et al. Interleukin 17 Promotes Angiotensin II-Induced Hypertension and Vascular Dysfunction. *Hypertension*. 2010;55(2):500-507.
12. Li Y, et al. γδT cell-derived interleukin-17A via an interleukin-1β- dependent mechanism mediates cardiac Injury and Fibrosis in hypertension. *Hypertension*. 2014;64(2):305-314.
13. Bastig T, Lazartigues E. DOCA-Salt Hypertension: an Update. *Curr hypertens reports*. 2017;19(4):32.
14. Amador CA, et al. Spironolactone decreases DOCA-salt-induced organ damage by blocking the activation of T helper 17 and the downregulation of regulatory T lymphocytes. *Hypertension* (Dallas, Tex : 1979). 2014;63(4):797-803.
15. Kvakan H, et al. Regulatory T Cells Ameliorate Angiotensin II–Induced Cardiac Damage. *Circulation*. 2009;119(22):2904-2912.
16. Kanellakis P, et al. CD4+CD25+Foxp3+ regulatory T cells suppress cardiac fibrosis in the hypertensive heart. *J Hypertens*. 2011;29(9):1820-1828.
17. Emmerson A, et al. Nox2 in regulatory T cells promotes angiotensin II–induced cardiovascular remodeling. *J Clin Invest*. 2018;128(7):3088-3101.
18. Giachini FR, et al. Extracellular signal-regulated kinase 1/2 activation, via downregulation of mitogen-activated protein kinase phosphatase 1, mediates sex differences in desoxycorticosterone acetate-salt hypertension vascular reactivity. *Hypertension* (Dallas, Tex : 1979). 2010;55(1):172-179.
19. Matrougui K, et al. Natural regulatory T cells control coronary arteriolar endothelial dysfunction in hypertensive mice. *Am J Pathol*. 2011;178(1):434-441.
20. Mian MOR, et al. Deficiency of T-regulatory cells exaggerates angiotensin II-induced microvascular injury by enhancing immune responses. *J Hypertens*. 2016;34(1):98-108.

21. Tinsley JH, et al. Interleukin-10 reduces inflammation, endothelial dysfunction, and blood pressure in hypertensive pregnant rats. *Am J Physiol Regul Integr Comp Physiol*. 2010;298(3):R713-R719.
22. Liu P, Sun M, Sader S. Matrix metalloproteinases in cardiovascular disease. *Can J Cardiol*. 2006;22(Suppl B):25B-30B.
23. Barhoumi T, et al. Matrix metalloproteinase-2 knockout prevents angiotensin II-induced vascular injury. *Cardiovasc Res*. 2017;113(14): 1753-1762.
24. Diaz-Canestro C, et al. MMP-2 knockdown blunts age-dependent carotid stiffness by decreasing elastin degradation and augmenting eNOS activation. *Cardiovasc Res*. 2021 Sep 29;cvab300
25. Visse R, Nagase H. Matrix metalloproteinases and tissue inhibitors of metalloproteinases: structure, function, and biochemistry. *Circ Res*. 2003;92(8):827-839.
26. Otto S, et al. A novel role of endothelium in activation of latent pro-membrane type 1 MMP and pro-MMP-2 in rat aorta. *Cardiovasc Res*. 2016;109(3):409-418.
27. Kopaliani I, et al. Cell-specific and endothelium-dependent regulations of matrix metalloproteinase-2 in rat aorta. *Basic Res Cardiol*. 2014;109(4):419.
28. Choi EY, et al. Developmental endothelial locus-1 is a homeostatic factor in the central nervous system limiting neuroinflammation and demyelination. *Mol Psychiatry*. 2014;20(7):880-888.
29. Choi EY, et al. Del-1, an endogenous leukocyte-endothelial adhesion inhibitor, limits inflammatory cell recruitment. *Science*. 2008;322(5904):1101-1104.
30. Hidai C, et al. Cloning and characterization of developmental endothelial locus-1: An embryonic endothelial cell protein that binds the alphavbeta3 integrin receptor. *Genes Dev*. 1998;12(1):21-33.
31. Subramanian P, et al. Endothelial cell-specific overexpression of developmental endothelial locus-1 does not influence atherosclerosis development in ApoE-/-mice. *Thromb Haemost*. 2017;117(10):2003-2005.
32. Mitroulis I, et al. Secreted protein Del-1 regulates myelopoiesis in the hematopoietic stem cell niche. *J Clin Invest*. 2017;127(10):3624-3639.
33. Shin J, et al. DEL-1 restrains osteoclastogenesis and inhibits inflammatory bone loss in nonhuman primates. Sci Trans Med. 2015;7(307):307ra155.
34. Eskan MA, et al. The leukocyte integrin antagonist Del-1 inhibits IL-17-mediated inflammatory bone loss. *Nat Immunol*. 2012;13(5):465-473.
35. Li X, et al. The DEL-1/β3 integrin axis promotes regulatory T cell responses during inflammation resolution. *J Clin Invest*. 2020;130(12):6261-6277.
36. Kourtzelis I, et al. DEL-1 promotes macrophage efferocytosis and clearance of inflammation. *Nat Immunol*. 2019;20(1):40-49.
37. Mitroulis I, et al. Leukocyte integrins: role in leukocyte recruitment and as therapeutic targets in inflammatory disease. *Pharmacol Ther*. 2015;147:123-135.
38. Tuna BG, Bakker ENTP, VanBavel E. Relation between active and passive biomechanics of small mesenteric arteries during remodeling. *J Biomech*. 2013;46(8):1420-1426.
39. Yadav VR, et al. Angiotensin II stimulation alters vasomotor response to adenosine in mouse mesenteric artery: Role for A1 and A2B adenosine receptors. *Br J Pharmacol*. 2015;172(20):4959-4969.

40. Nagareddy PR, et al. Inhibition of matrix metalloproteinase-2 improves endothelial function and prevents hypertension in insulin-resistant rats. *Br J Pharmacol*. 2012;165(3):705-715.
41. Krishnan SM, et al. Inflammasome activity is essential for one kidney/deoxycorticosterone acetate/salt-induced hypertension in mice. *Br J Pharmacol*. 2016;173(4):752-765
42. Chen L-S, et al. Endothelial Cell–Specific Overexpression of Del-1 Drives Expansion of Haematopoietic Progenitor Cells in the Bone Marrow. *Thromb Haemost*. 2018;118:613–616.
43. Kourtzelis I, et al. Developmental endothelial locus-1 modulates platelet-monocyte interactions and instant blood-mediated inflammatory reaction in islet transplantation. *Thromb Haemost*. 2016;115(4):781-788.
44. Riedel K, et al. Estrogen determines sex differences in adrenergic vessel tone by regulation of endothelial β-adrenoceptor expression. *Am J Physiol Heart Circ Physiol*. 2019;317(2):H243-H254.
45. Al-Gburi S, et al. Sex-specific differences in age-dependent progression of aortic dysfunction and related cardiac remodeling in spontaneously hypertensive rats. *Am J Physiol Regul Integr Comp Physiol*. 2017;312:R835–R849 312.
46. Martin M, et al. Antihypertensive and cardioprotective effects of the dipeptide isoleucine-tryptophan and whey protein hydrolysate. *Acta Physiol*. 2015;215(4):167-76.

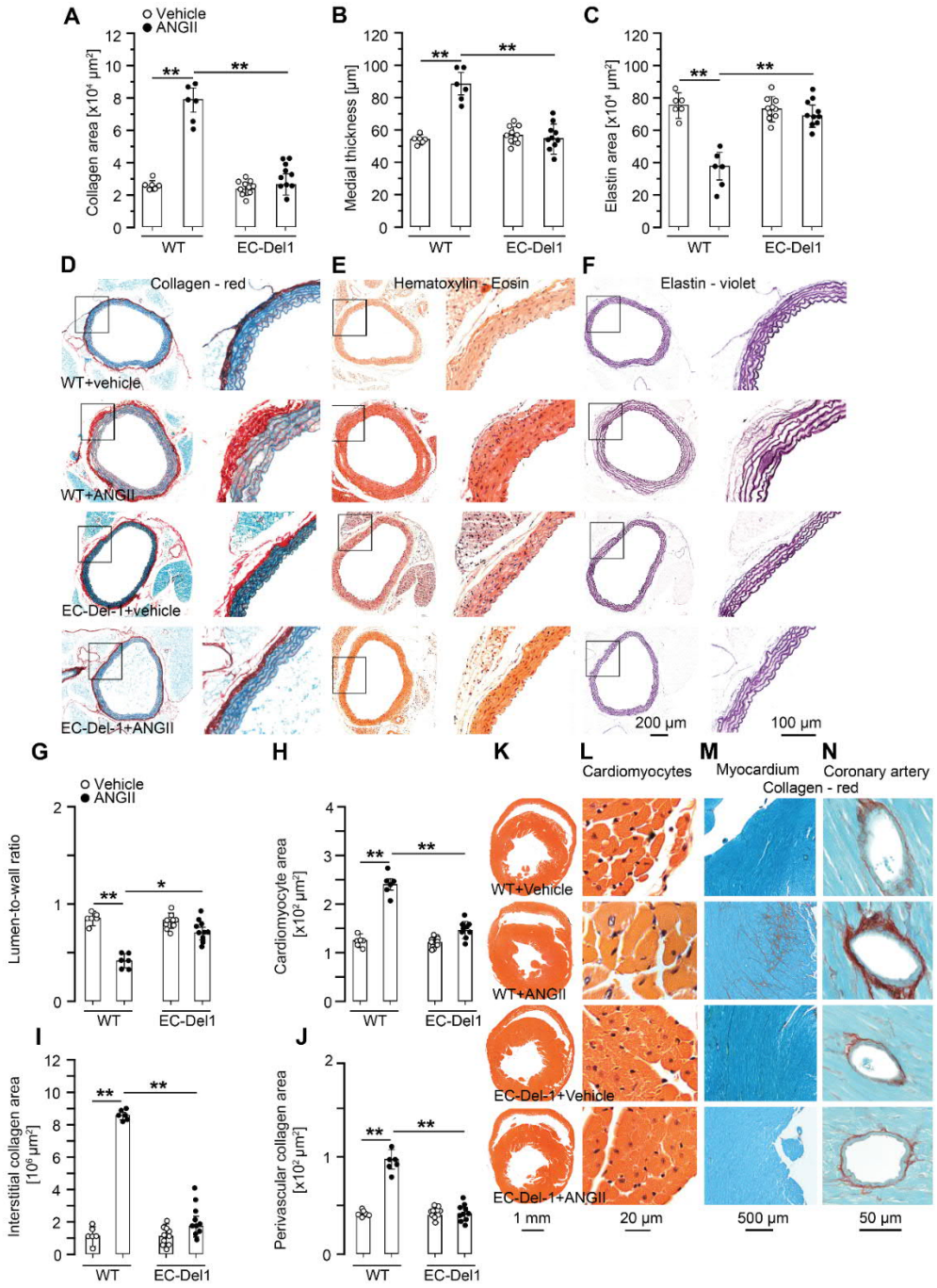

Figure 1. EC-Del1 mice are protected from ANGII-induced cardiovascular remodeling. 1.5 mg/kg/day ANGII or vehicle was infused in EC-Del1 and WT littermates for 4-weeks. Histological stainings and analysis of aortic adventitial collagen **(A, D)**, medial wall thickness (**B, E)** and medial elastin **(C, F)** on the 28th day of ANGII or vehicle infusion. Histological stainings and analysis of cardiac lumen-to-wall ratio **(G, K)**, cardiomyocyte cross-sectional area **(H, L)**, interstitial **(I, M)** and perivascular coronary **(J, N)** collagen (n=6-10 mice per group). Data represent mean ± SEM. **P*<0.05, ***P*<0.01 analyzed by two-way ANOVA with Bonferroni post hoc test to adjust for multiple comparisons.

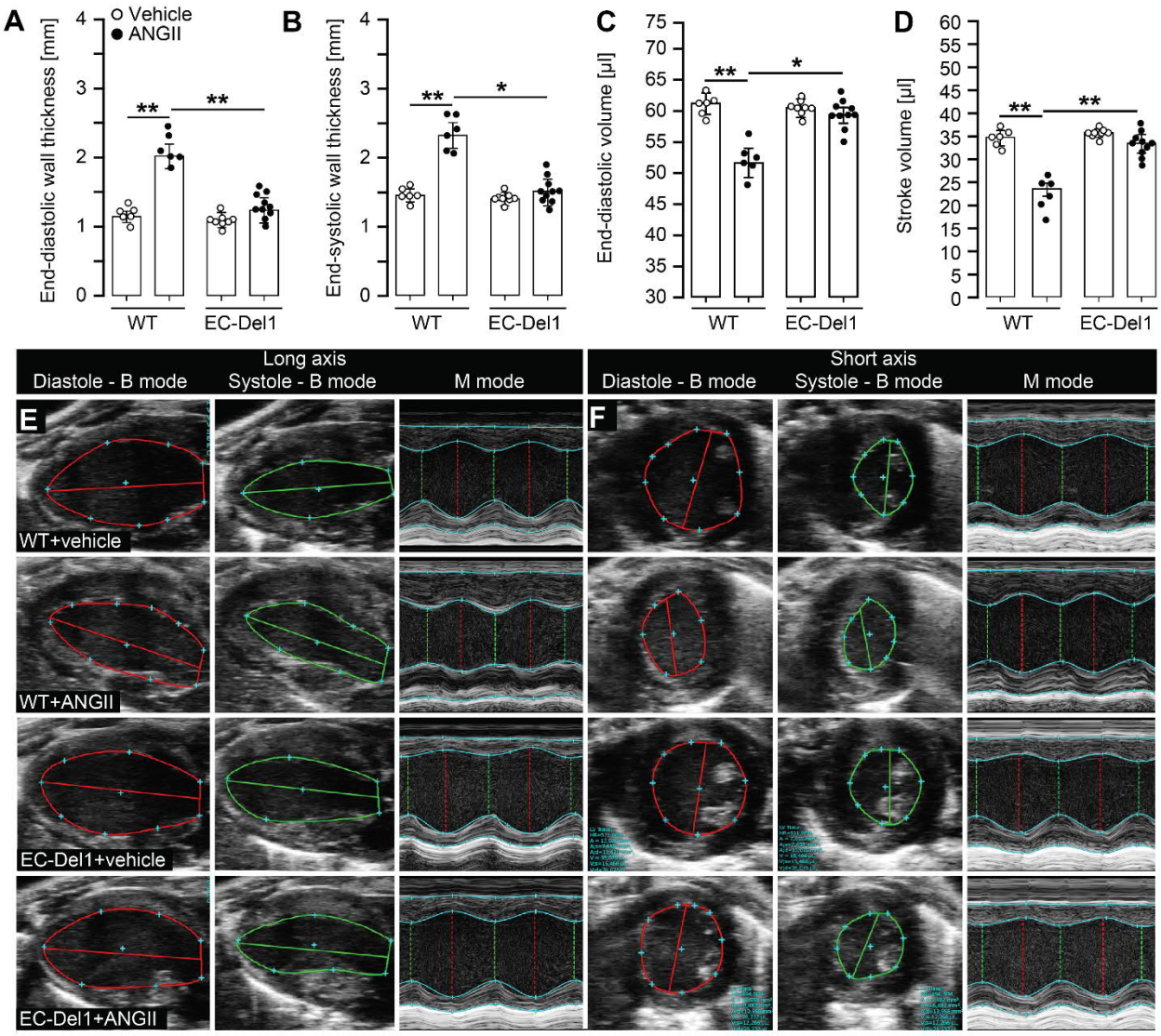

Figure 2. EC-Del1 mice are protected from ANGII-induced concentric cardiomyopathy. Echocardiographic evaluation and analysis of structural and hemodynamic parameters of concentric cardiomyopathy, cardiac end-diastolic **(A)** and end-systolic wall thickness **(B)**, end-diastolic **(C)** and stroke volumes **(D)**. Representative echocardiographic images of B and M modes of long **(E)** and short axis **(F)**. The parameters of concentric cardiomyopathy were analyzed in long axis (n=6-10 mice per group). Data represent mean ± SEM. **P*<0.05, ***P*<0.01 analyzed by two-way ANOVA with Bonferroni post hoc test to adjust for multiple comparisons.

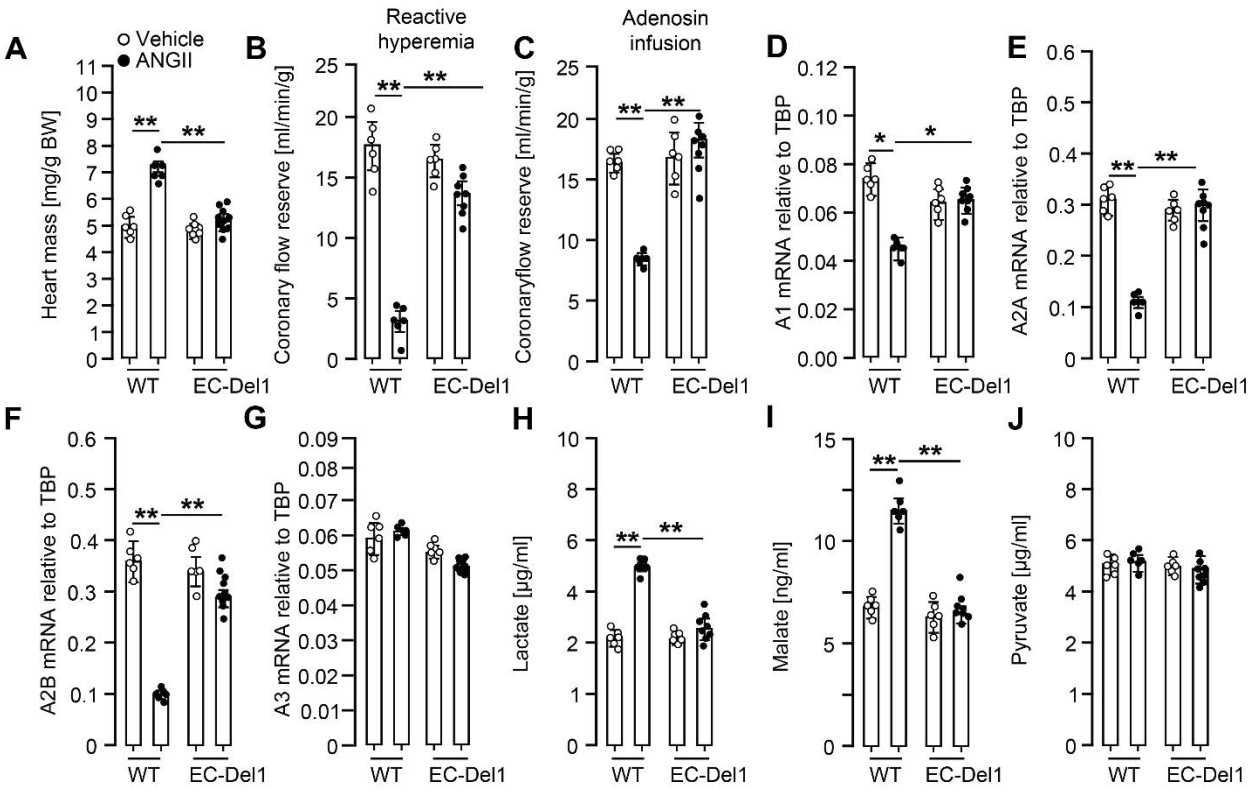

Figure 3. EC-Del1 mice are protected from ANGII-induced worsening of the coronary flow and metabolic adaptation. Heart mass after 28-days of ANGII infusion **(A)** and coronary flow reserve assessed after flow stop **(B)** or adenosine infusion **(C)**. mRNA levels of cardiac adenosine receptors A1, A2A, A2B and A3 **(D-G)**. Metabolites of glycolysis, lactate **(H)** and malate **(I)**, along with pyruvate **(J)** (n=6-10 mice per group). Data represent mean ± SEM. **P*<0.05, ***P*<0.01 analyzed by two-way ANOVA with Bonferroni post hoc test to adjust for multiple comparisons.

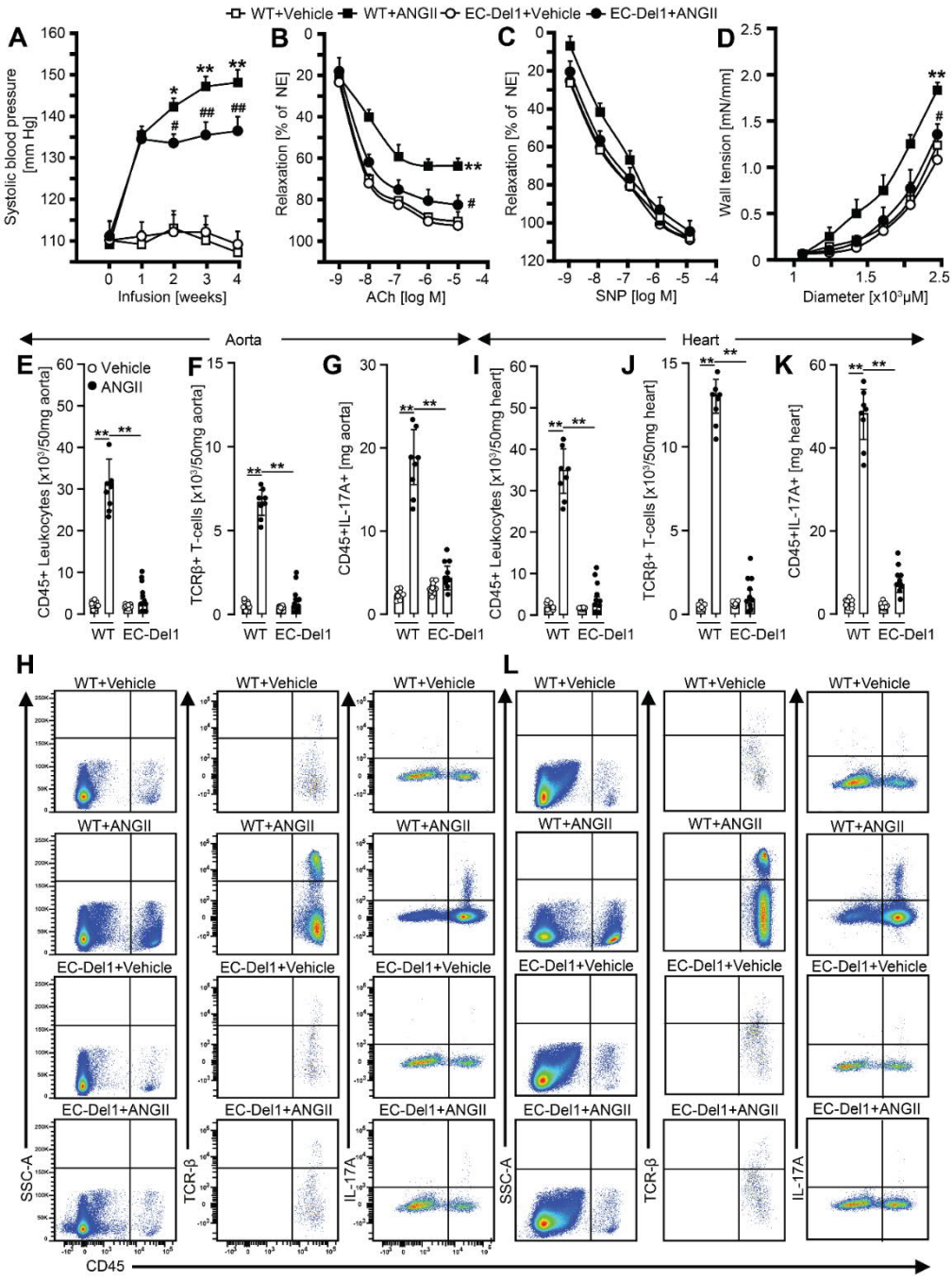

Figure 4. EC-Del1 mice are protected from ANGII-dependent progression of hypertension, arterial stiffness and cardiovascular inflammation. Systolic blood pressure **(A)**, ACh mediated endothelium-dependent and -independent aortic relaxations **(B, C)** and aortic passive tension development **(D)** after 4-weeks of ANGII- or vehicle-infusion. FACS diagrams and plots of CD45+ leukocytes, TCRβ+ T-cells and CD45+IL17A+ cells in aorta **(E-H)** and heart **(I-L)** (A, n=12, B-D n=10, E-L n=8-10 mice per group). Data represent mean ± SEM. **P*<0.05 (vs. WT+vehicle in A), #*P*<0.05 (vs. WT+ANGII in A-D), ***P*<0.01 (vs. WT+vehicle in A-D), ##*P*<0.05 (vs. WT+ANGII in A-D) analyzed by two-way ANOVA (panels A-D for repeated measures) with Bonferroni post hoc test to adjust for multiple comparisons.

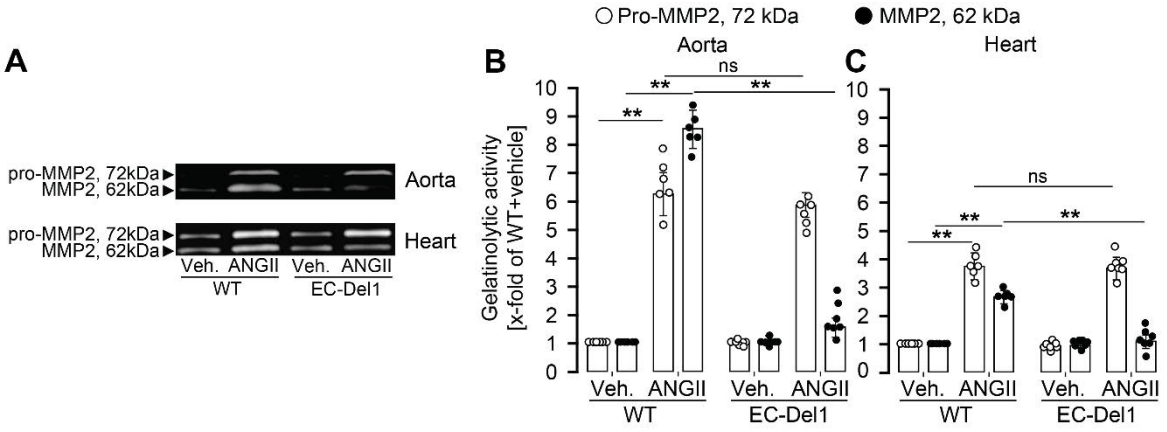

Figure 5. EC-Del1 mice have low MMP2 activity in cardiovascular tissues. Levels of latent pro-MMP2 and active MMP2 in aorta **(A, B)** and heart **(A, C)** after 4-weeks of ANGII- or vehicle-infusion (n=6-7 mice per group). Data represent mean ± SEM. **P*<0.05, ***P*<0.01 analyzed by two-way ANOVA with Bonferroni post hoc test to adjust for multiple comparisons.

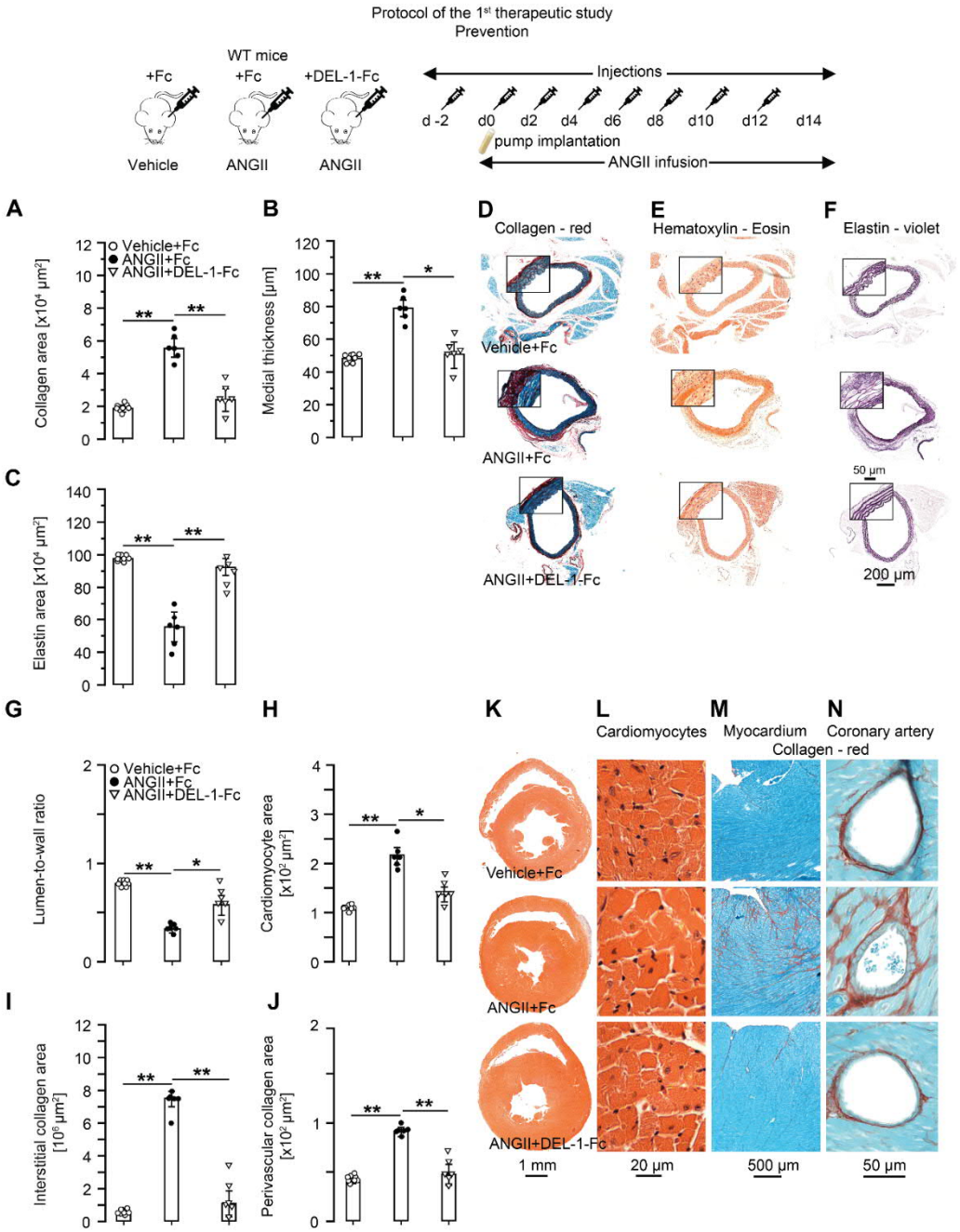

Figure 6. Treatment with DEL-1-Fc starting before established hypertension prevents cardiovascular remodeling. Two days before starting the ANGII-infusion, 30 µg of DEL-1-Fc or Fc alone was injected in WT mice. Following injections were performed at the day of ANGII pump implantations and every second day up to 12th day of infusion. Histological stainings and analysis of aortic adventitial collagen **(A, D)**, medial wall thickness (**B, E)** and medial elastin **(C, F)**. Histological stainings and analysis of LV lumen-to-wall ratio **(G, K)**, cardiomyocyte cross-sectional area **(H, L)**, interstitial **(I, M)** and perivascular coronary **(J, N)** collagen (n=6-8 mice per group). Data represent mean ± SEM. **P*<0.05, ***P*<0.01 analyzed by one-way ANOVA with Bonferroni post hoc test to adjust for multiple comparisons.

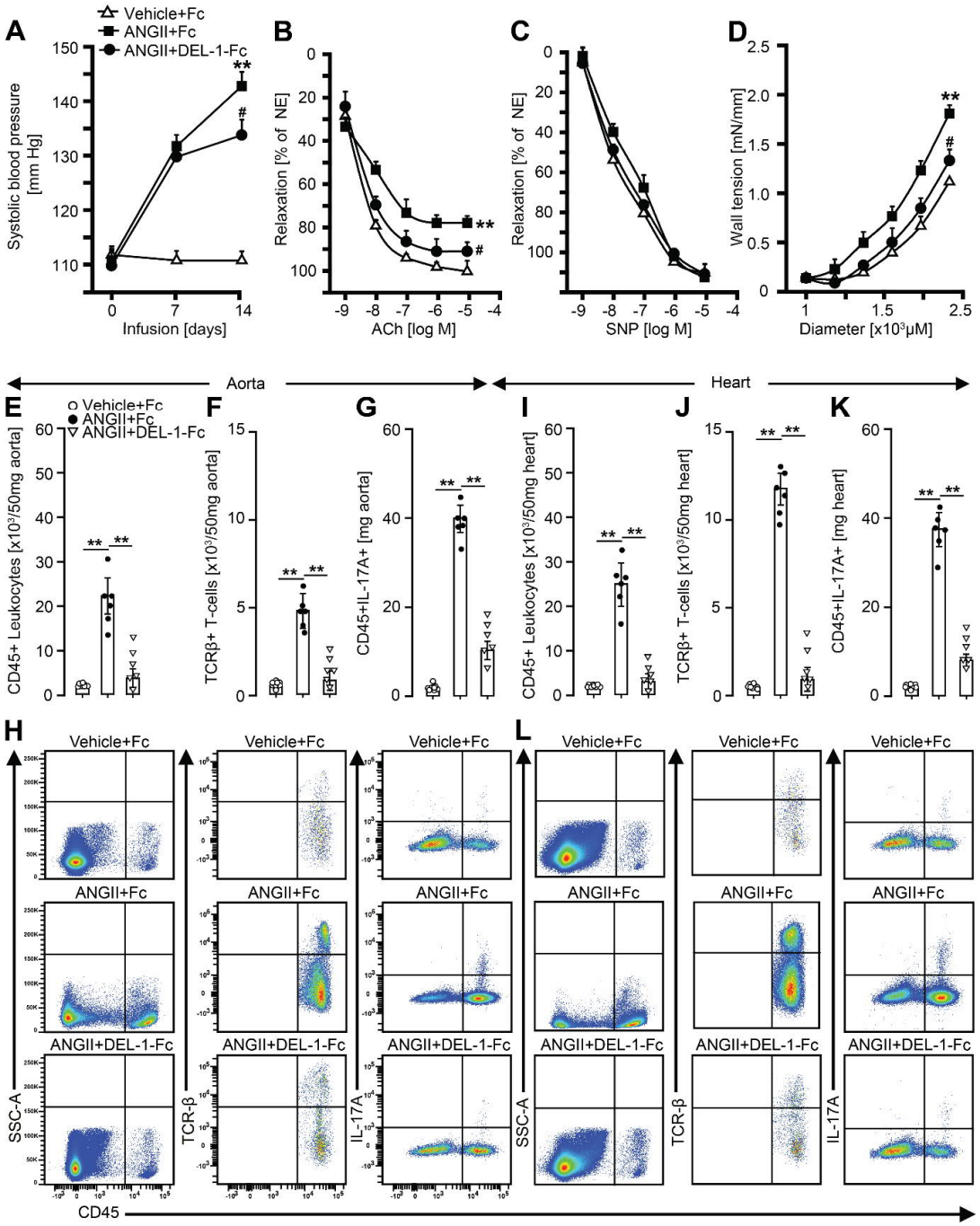

Figure 7. Treatment with DEL-1-Fc starting before established hypertension prevents progression of SBP, arterial stiffness and cardiovascular inflammation. Systolic blood pressure **(A)**, ACh mediated endothelium-dependent and -independent aortic relaxations **(B, C)** and aortic passive tension development **(D)** after 2-weeks of ANGII- or vehicle-infusion with DEL-1-Fc or Fc treatment. FACS diagrams and plots of CD45+ leukocytes, TCRβ+ T-cells and CD45+IL17A+ cells in aorta **(E-H)** and heart **(I-L)** (n=6-8 mice per group). Data represent mean ± SEM. $^{\#}P<0.05$ (vs. WT+ANGII in A-D), $^{**}P<0.01$ (vs. WT+vehicle in A-D), $^{\#\#}P<0.05$ (vs. WT+ANGII in A-D) analyzed by one-way ANOVA (panels A-D for repeated measures) with Bonferroni post hoc test to adjust for multiple comparisons.

Figure 8

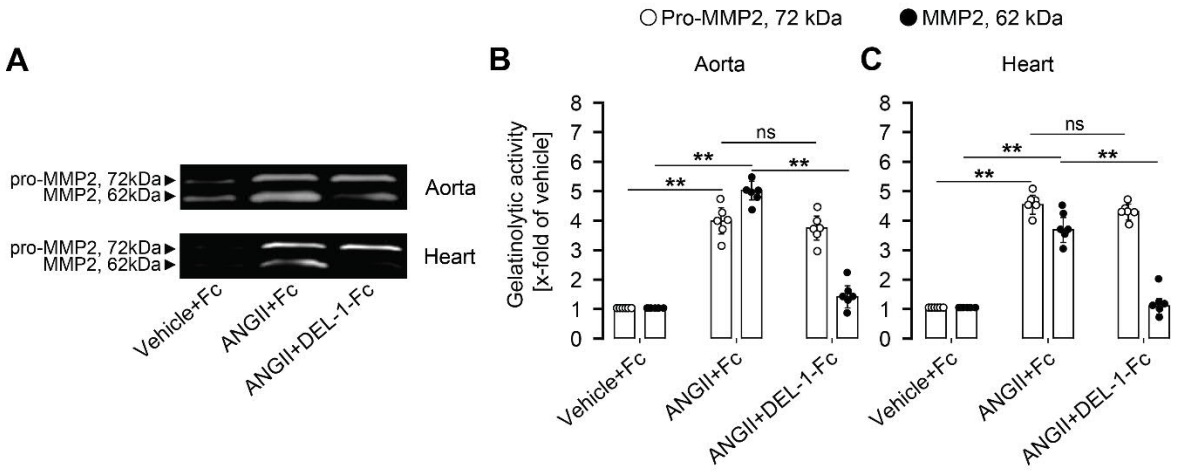

Figure 8. DEL-1-Fc treated mice have low MMP2 activity in aorta and heart. Levels of latent pro-MMP2 and active MMP2 in aorta **(A, C)** and heart **(B, C)** (n=6 mice per group). Data represent mean ± SEM. **P*<0.05, ***P*<0.01 analyzed by one-way ANOVA with Bonferroni post hoc test to adjust for multiple comparisons.

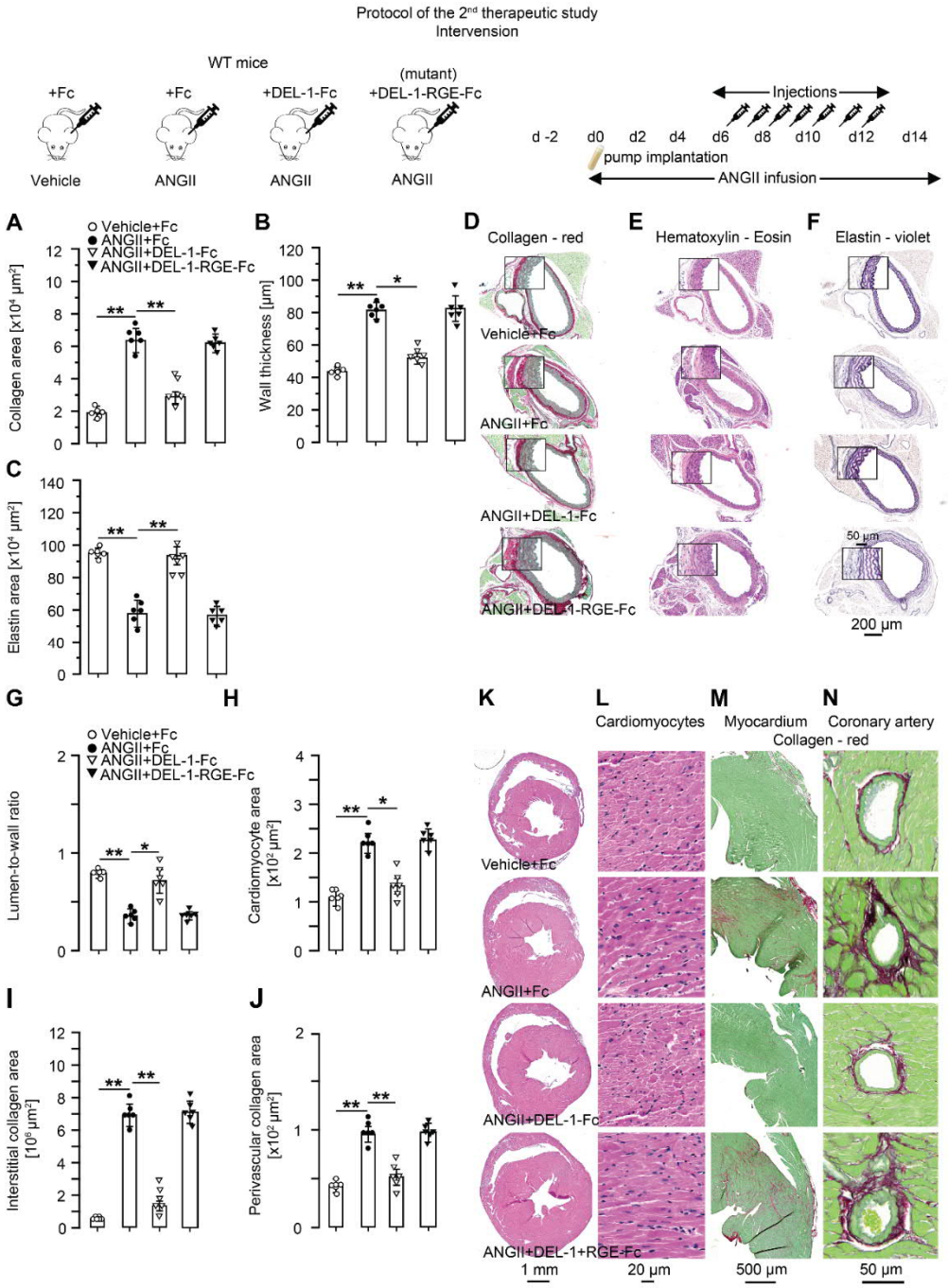

Figure 9. Treatment with DEL-1-Fc, but not DEL-1-RGE-Fc starting after established hypertension abrogates cardiovascular remodeling in ANGII-induced hypertension. On the 6th day after starting the ANGII-infusion, 20 µg of DEL-1-Fc, Del-RGE-Fc or Fc alone was injected. Following injections were performed every day up to the 12th day of ANGII infusion. Histological stainings and analysis of aortic adventitial collagen **(A, D)**, medial wall thickness (**B, E)** and medial elastin **(C, F)**. Histological stainings and analysis of cardiac lumen-to-wall ratio **(G, K)**, cardiomyocyte cross-sectional area **(H, L)**, interstitial **(I, M)** and perivascular coronary **(J, N)** collagen (n=6 mice per group). Data are means ± SE. **P*<0.05, ***P*<0.01 analyzed by one-way ANOVA with Bonferroni post hoc test to adjust for multiple comparisons.

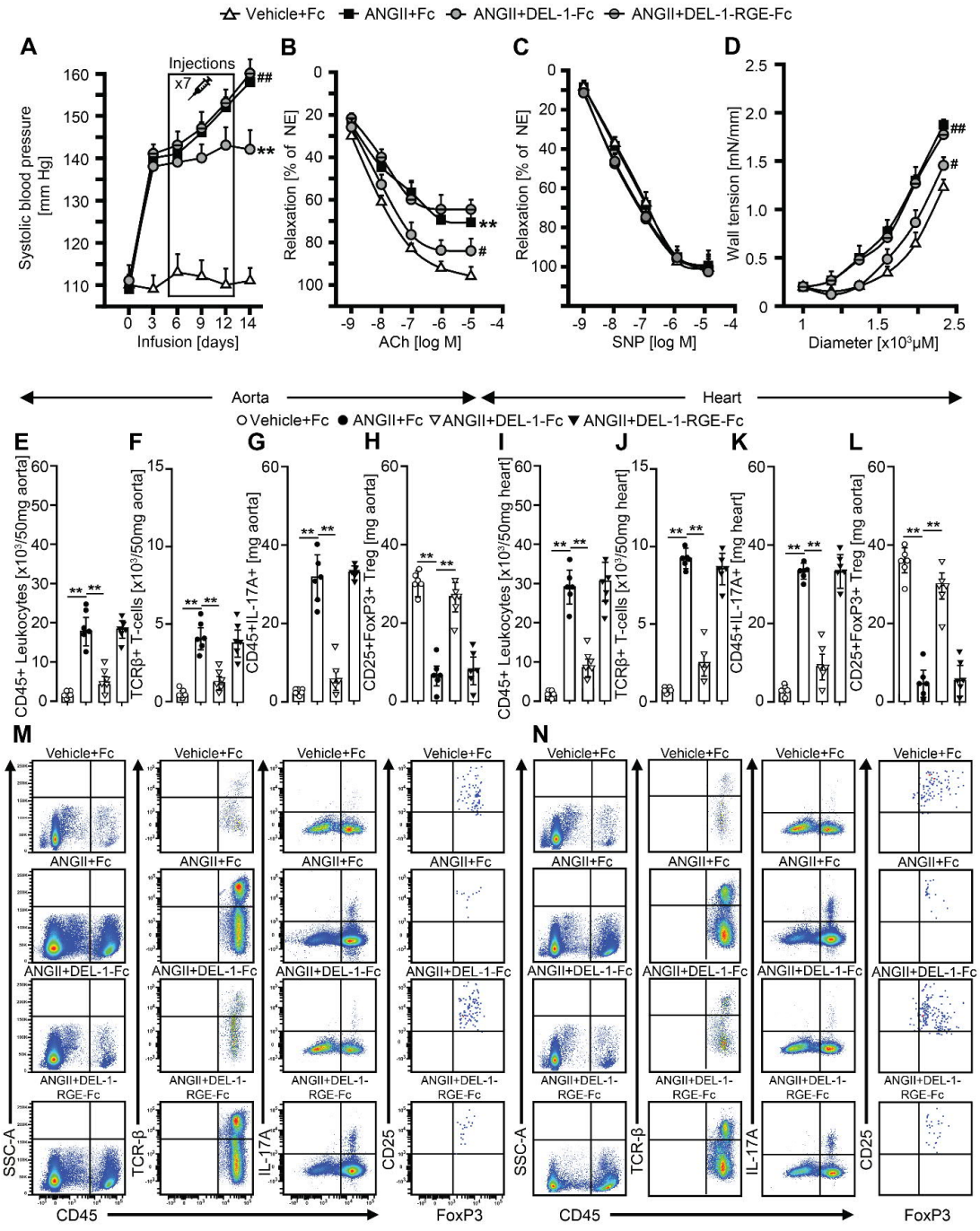

Figure 10. Treatment with DEL-1-Fc, but not DEL-1-RGE-Fc starting after established hypertension abrogates progression of SBP, arterial stiffness, cardiovascular inflammation and stabilizes anti-inflammatory Treg cell numbers. Systolic blood pressure **(A)**, endothelium-dependent (ACh) and -independent (SNP) aortic relaxations **(B, C)** and aortic passive tension development **(D)** after 2-weeks of ANGII- or vehicle-infusion with DEL-1-Fc, DEL-1-RGE-Fc or Fc treatments. FACS diagrams and plots of CD45+ leukocytes, TCRβ+ T-cells, CD45+IL17A+ and CD25+FoxP3+ Treg cells in aorta **(E-H, M)** and heart **(I-L, N)** (n=6 mice per group). Data are means ± SE. $^{\#}P<0.05$ (vs. WT+ANGII in B-D), $^{**}P<0.01$ (vs. WT+vehicle in A-B), $^{\#\#}P<0.05$ (vs. WT+ANGII in A, D) analyzed by one-way ANOVA (panels A-D for repeated measures) with Bonferroni post hoc test to adjust for multiple comparisons.

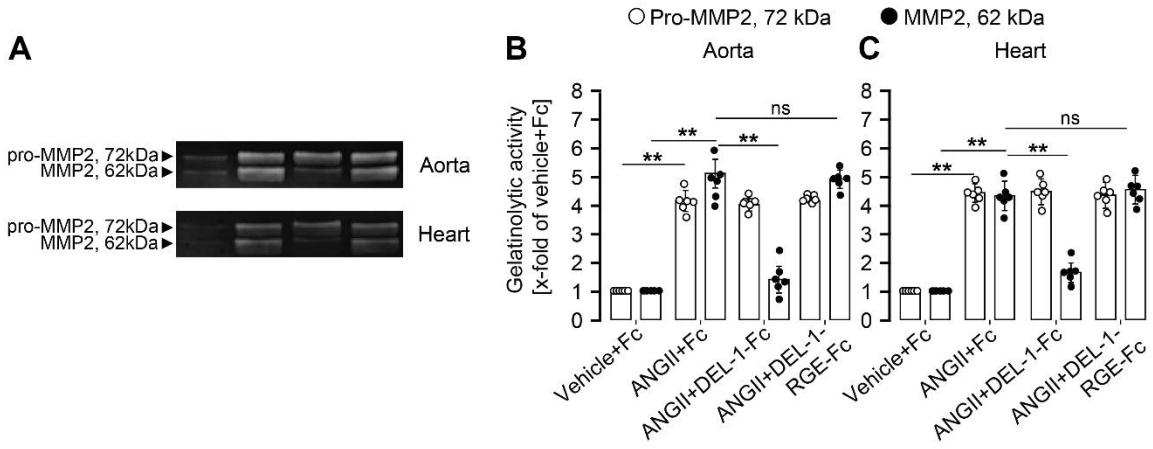

Figure 11. DEL-1-Fc, but not DEL-1-RGE-Fc treated mice have low MMP2 activity in aorta and heart. Levels of latent pro-MMP2 and active MMP2 in aorta **(A, C)** and heart **(B, C)** (n=6 mice per group). Data are means ± SE. **P*<0.05, ***P*<0.01 analyzed by one-way ANOVA with Bonferroni post hoc test to adjust for multiple comparisons.

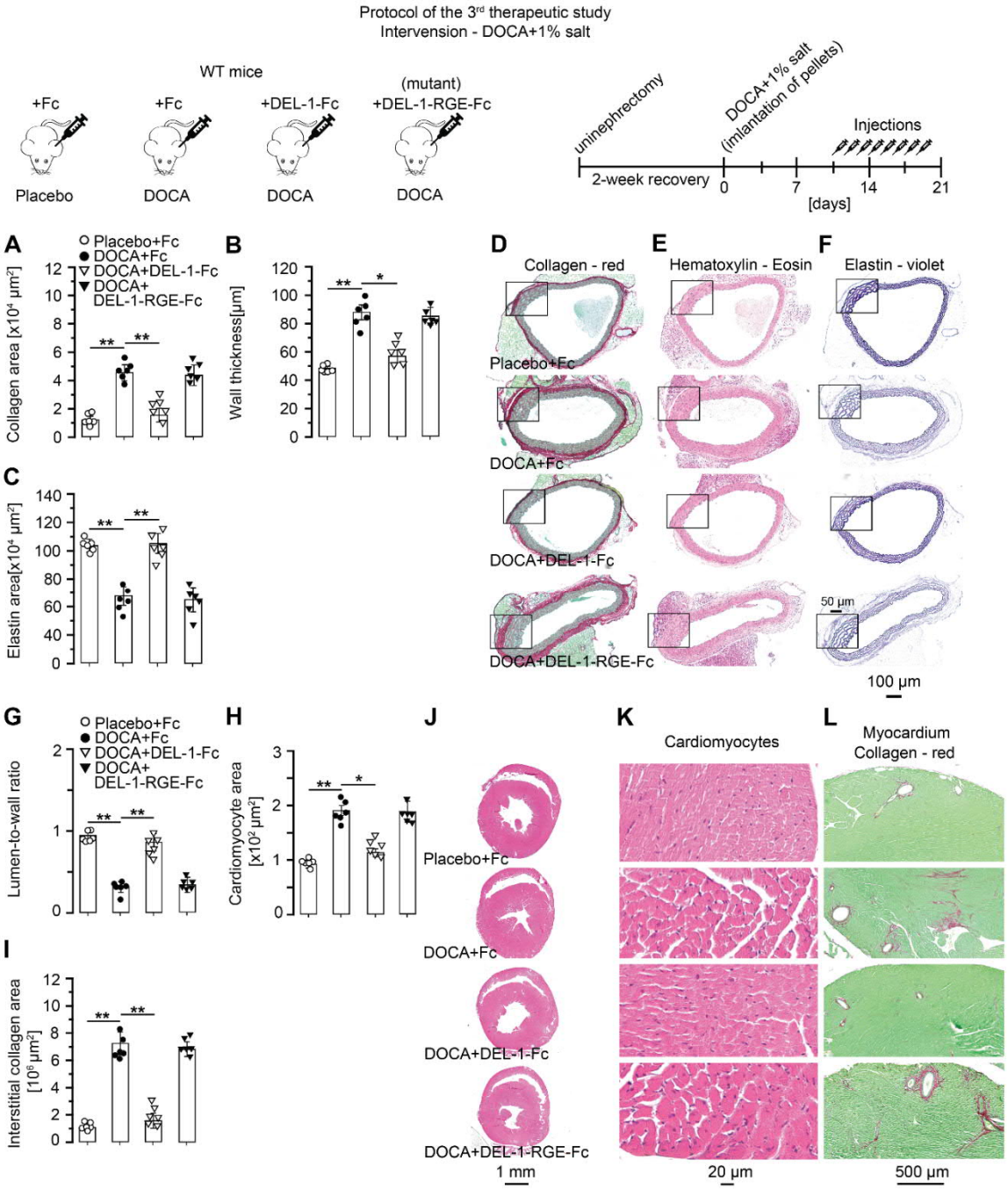

Figure 12. Treatment with DEL-1-Fc, but not DEL-1-RGE-Fc starting after established hypertension abrogates cardiovascular remodeling in DOCA-salt hypertension. On the 10th day after implantation of DOCA pellets, 20 µg of DEL-1-Fc, Del-RGE-Fc or Fc alone was injected. A total of eight injections up to the 18th day were performed. Histological stainings and quantification of aortic adventitial collagen **(A, D)**, medial wall thickness (**B, E)** and medial elastin **(C, F)**. Histological stainings and quantification of cardiac lumen-to-wall ratio **(G, J)**, cardiomyocyte cross-sectional area **(H, K)** and interstitial **(I, L)** collagen (n=6 mice per group). Data are means ± SE. **P*<0.05, ***P*<0.01 analyzed by one-way ANOVA with Bonferroni post hoc test to adjust for multiple comparisons.

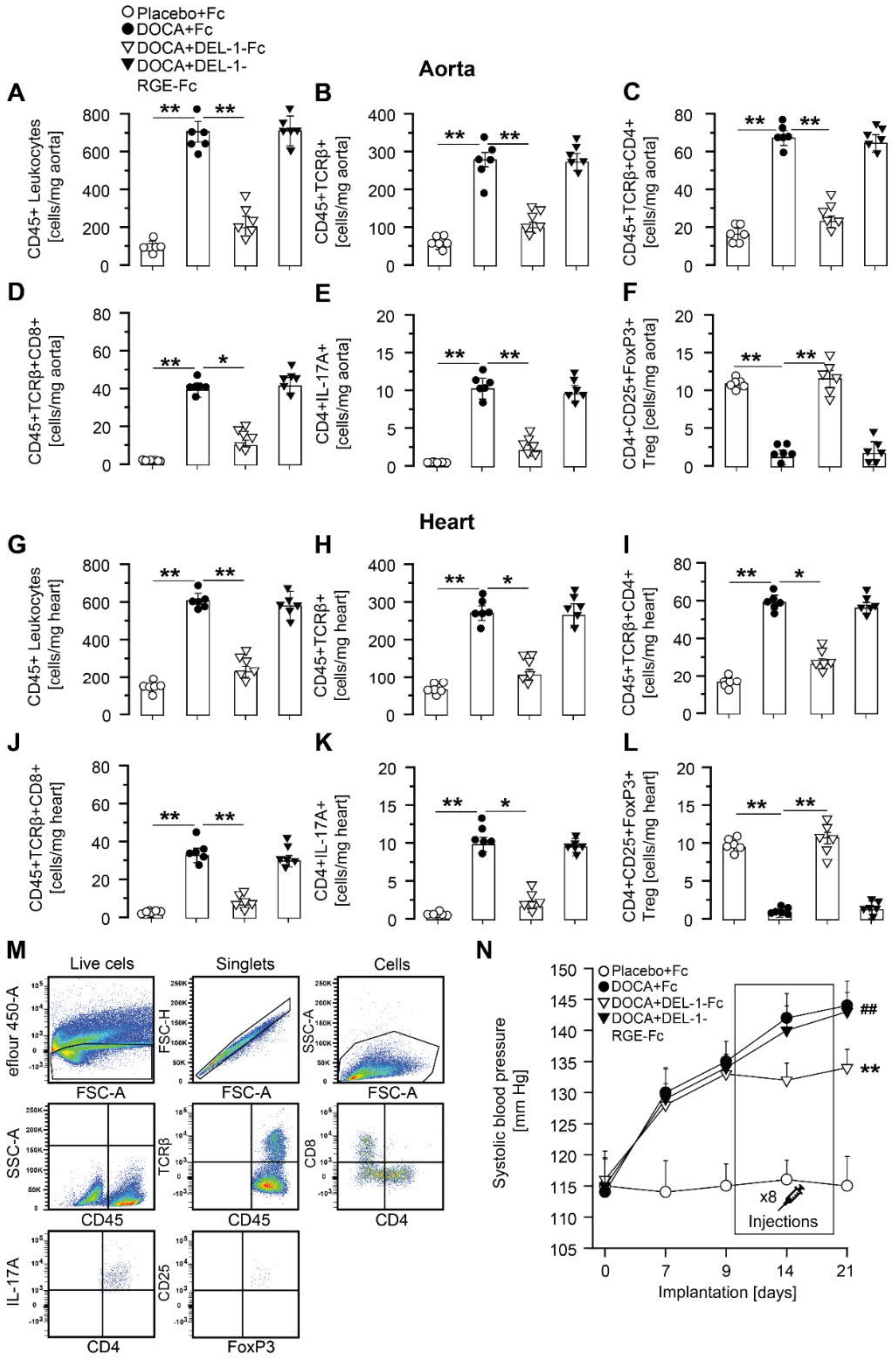

Figure 13. Treatment with DEL-1-Fc, but not DEL-1-RGE-Fc starting after established DOCA-salt-induced hypertension abrogates progression of SBP, arterial stiffness, cardiovascular inflammation and stabilizes anti-inflammatory Treg cell numbers. FACS diagrams of inflammatory cells in aorta **(A-F)** and heart **(G-L)**. Systolic blood pressure development up to 21 days of DOCA-salt hypertension **(N).** Representative gating strategy for CD45+, CD45+TCRβ+, CD45+TCRβ+CD4+, CD45+TCRβ+CD8+, CD4+IL-17A+ and CD4+CD25+FoxP3+ cells **(M)**. (n=6 mice per group). Data are means ± SE. **P*<0.05, ***P*<0.01 analyzed by one-way ANOVA (panel Z for repeated measures) with Bonferroni post hoc test to adjust for multiple comparisons.

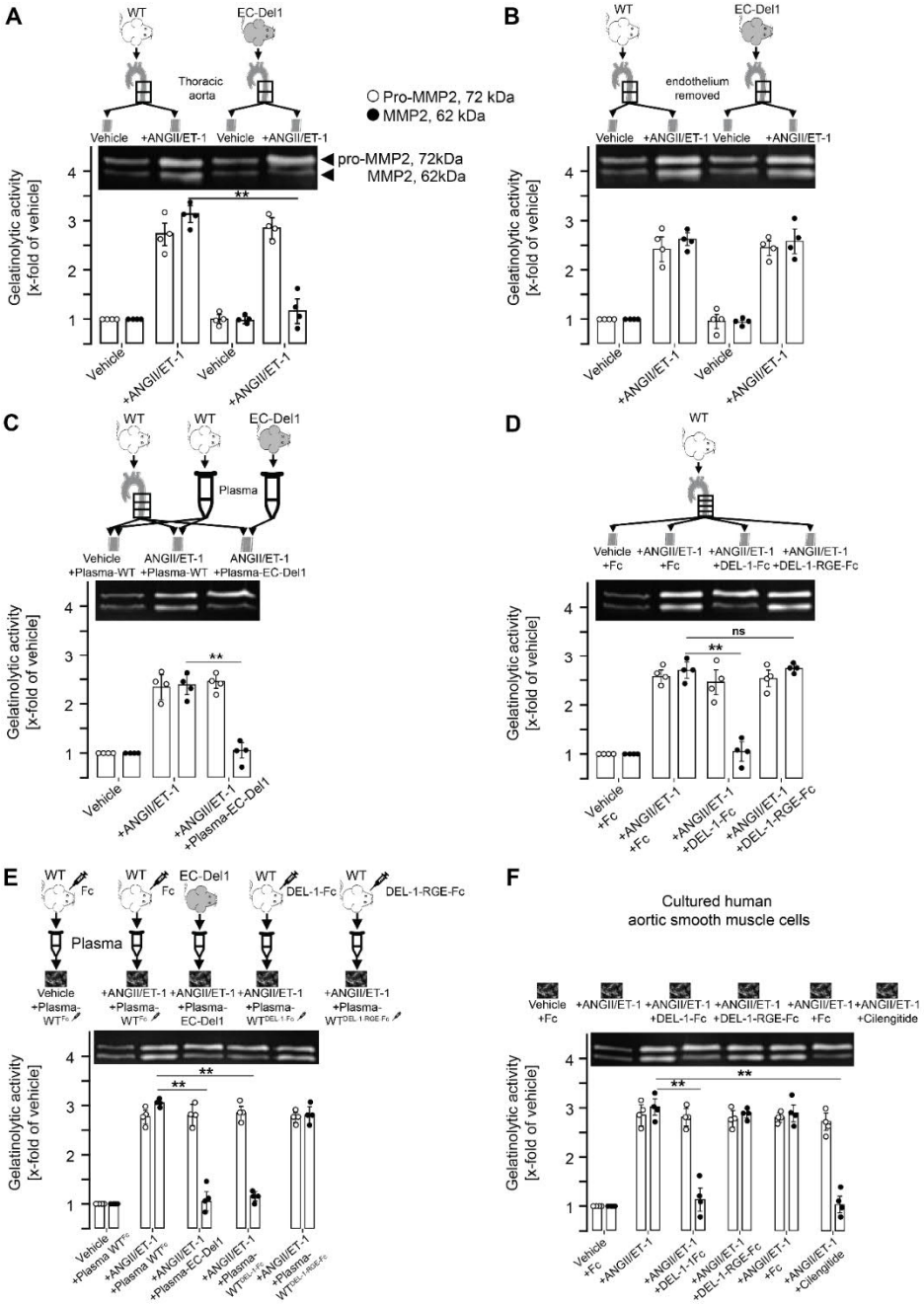

Figure 14. DEL-1-inhibits αvβ3-integrin-dependent activation of latent pro-MMP2. Thoracic aorta was isolated from WT and EC-Del1 mice and stimulated with ANGII/ET1 followed by assessment of latent pro- and active MMP2 **(A)**. Stimulation of isolated aorta from WT and EC-Del1 mice without endothelium **(B)**. ANGII/ET1 stimulated aortas of WT mice pretreated with Fc, DEL-1-Fc or DEL-1-RGE-Fc **(C)**. ANGII/ET1 stimulated aortas of WT mice pretreated with plasma of EC-Del1 mice **(D)**. Cultured human aortic smooth muscle cells pretreated with plasmas of WT mice injected with Fc, DEL-1-Fc, DEL-1-RGE-Fc or plasma of EC-Del1 mice and then stimulated with ANGII/ET1 **(E)**. Cultured human aortic smooth muscle cells pretreated with Fc, DEL-1-Fc, DEL-1-RGE-Fc or pharmacological αvβ3-integrin cilengitide and then stimulated with ANGII/ET1 **(F)** (A-F n=4 independent experiments). Data represent mean ± SEM. $^{**}P<0.01$ analyzed by one-way ANOVA with Bonferroni post hoc test to adjust for multiple comparisons.

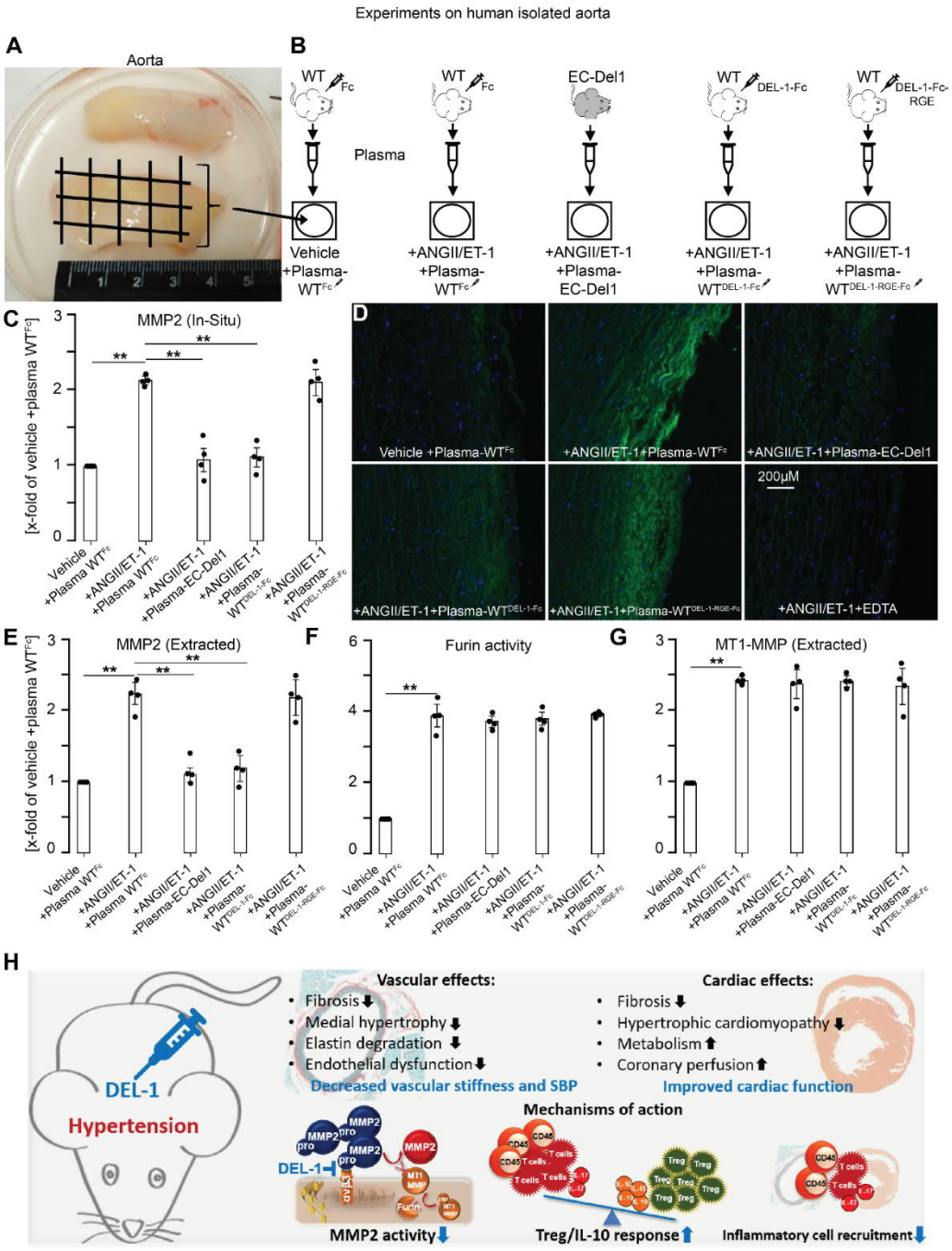

Figure 15. DEL-1-inhibits αvβ3-integrin-dependent activation of latent pro-MMP2 in isolated human aorta. A piece of isolated human aorta, which was divided in smaller 5 x 5 mm^2 pieces and incubated in tissue well-plates followed by pretreatment with plasmas of Fc, DEL-1-Fc, DEL-1-RGE-Fc injected mice or plasma of EC-Del1 mice and then stimulated with ANGII/ET1 **(A, B)**. In-situ gel Zymography showing MMP2 activity in isolated human aorta **(C, D)**. MMP2 **(E)**, furin **(F)** and MT1-MMP **(G)** activity assays in extracts of isolated human aorta. Schematic summary of protective effects and anti-inflammatory mechanisms of action of DEL-1 in ANGII-induced hypertension and cardiovascular remodeling **(H)** (A-G n=4 independent experiments). Data represent mean ± SEM. ** P<0.01 analyzed by one-way ANOVA with Bonferroni post hoc test to adjust for multiple comparisons.